Journal of Contaminant Hydrology 167 (2014) 1–22

Contents lists available at ScienceDirect

Journal of Contaminant Hydrology

journal homepage: www.elsevier.com/locate/jconhyd

Potential migration of buoyant LNAPL from Intermediate Level Waste (ILW) emplaced in a geological disposal facility (GDF) for UK radioactive waste

Steven J. Benbow [a,*], Michael O. Rivett [b], Neil Chittenden [b], Alan W. Herbert [b], Sarah Watson [a], Steve J. Williams [c], Simon Norris [c]

[a] Quintessa Limited, Henley-on-Thames, Oxfordshire RG9 1AY, UK
[b] Water Sciences Research Group, School of Geography, Earth & Environmental Sciences, University of Birmingham, Birmingham B15 2TT, UK
[c] Nuclear Decommissioning Authority Radioactive Waste Management Directorate (NDA RWMD), now Radioactive Waste Management Limited (RWM), B587, Curie Avenue, Harwell Campus, Didcot, Oxon OX11 0RH, UK

ARTICLE INFO

Article history:
Received 11 March 2014
Received in revised form 18 July 2014
Accepted 21 July 2014
Available online 1 August 2014

Keywords:
Intermediate Level Waste (ILW)
Geological disposal facility (GDF)
Light non-aqueous phase liquid (LNAPL)
Multiphase flow
Numerical model
Radioactive waste disposal safety case

ABSTRACT

A safety case for the disposal of Intermediate Level (radioactive) Waste (ILW) in a deep geological disposal facility (GDF) requires consideration of the potential for waste-derived light non-aqueous phase liquid (LNAPL) to migrate under positive buoyancy from disposed waste packages. Were entrainment of waste-derived radionuclides in LNAPL to occur, such migration could result in a shorter overall travel time to environmental or human receptors than radionuclide migration solely associated with the movement of groundwater. This paper provides a contribution to the assessment of this issue through multiphase-flow numerical modelling underpinned by a review of the UK's ILW inventory and literature to define the nature of the associated ILW LNAPL source term. Examination has been at the waste package–local GDF environment scale to determine whether proposed disposal of ILW would lead to significant likelihood of LNAPL migration, both from waste packages and from a GDF vault into the local host rock. Our review and numerical modelling support the proposition that the release of a discrete free phase LNAPL from ILW would not present a significant challenge to the safety case even with conservative approximations. 'As-disposed' LNAPL emplaced with the waste is not expected to pose a significant issue. 'Secondary LNAPL' generated in situ within the disposed ILW, arising from the decomposition of plastics, in particular PVC (polyvinyl chloride), could form the predominant LNAPL source term. Released high molecular weight phthalate plasticizers are judged to be the primary LNAPL potentially generated. These are expected to have low buoyancy-based mobility due to their very low density contrast with water and high viscosity. Due to the inherent uncertainties, significant conservatisms were adopted within the numerical modelling approach, including: the simulation of a deliberately high organic material — PVC content wastestream (2D03) within an annular grouted waste package vulnerable to LNAPL release; upper bound inventory estimates of LNAPLs; incorporating the lack of any hydraulic resistance of the package vent; the lack of any degradation of dissolved LNAPL; and, significantly, the small threshold displacement pressure assumed at which LNAPL is able to enter initially water-saturated pores. Initial scoping calculations on the latter suggested that the rate at which LNAPL is able to migrate from a waste package is likely to be very small and insignificant for likely representative displacement pressure data: this represents a key result. Adopting a conservative displacement pressure, however, allowed the effect of other features and processes in the system to be assessed. High LNAPL viscosity together with low density contrast with water reduces LNAPL migration potential. Migration to the host rock is less

* Corresponding author. Tel.: +44 1491 636246.
E-mail address: stevenbenbow@quintessa.org (S.J. Benbow).

http://dx.doi.org/10.1016/j.jconhyd.2014.07.011

likely if waste package vent fluxes are small, solubility limits are high and path lengths through the backfill are short. The capacity of the system to dissolve all of the free LNAPL will, however, depend on groundwater availability. Even with the conservatisms invoked, the overall conclusion of model simulations of intact and compromised (cracked or corroded) waste packages, for a range of realistic ILW LNAPL scenarios, is that it is unlikely that significant LNAPL would be able to migrate from the waste packages and even more unlikely it would be sufficiently persistent to reach the host rock immediately beyond the GDF.

1. Introduction

Building a safety case for the disposal of Intermediate Level (radioactive) Waste (ILW) in a deep geological disposal facility (GDF) requires consideration of potential pathways by which radionuclides might be returned to the accessible environment. Alongside consideration of radionuclide transport within any groundwater (Altmann, 2008; Grambow, 2008), it is important to evaluate the impact of other potentially mobile fluids that might be disposed to, or generated within, the GDF – for example gas, generated by corrosion and microbial degradation (NDA, 2010a) and buoyant light non-aqueous phase liquid (LNAPL) – on the overall evolution of a disposal system's performance. The potential impact of LNAPL has been identified in the recent past as a viability issue for a GDF by several authors (Askarieh et al., 1993; Rees et al., 2002; United Kingdom Nirex Limited (Nirex), 2005; Wealthall, 2002). A safety case should address the concern that any buoyant LNAPL might migrate from the waste packages and could result in a shorter overall travel time to environmental or human receptors for any entrained radionuclides, in comparison with radionuclide migration solely associated with the movement of groundwater.

Our work herein focuses upon the initial part of this pathway — the waste package and the 'near field' of a GDF vault (waste stacks and backfill material). It aims to address the key question: is there a significant safety case issue associated with LNAPL in relation to radionuclides migrating from a disposal vault? Our study does not attempt to assess LNAPL migration through the geological barrier to surface, but does aim to inform on the need for such assessment.

In common with more conventional contaminated land LNAPL sources, the ILW LNAPL source poses both saturation-based and composition-based risks (ITRC, 2009). Saturation-based risk is driven by the amount (saturation) of LNAPL present and its potential to result in LNAPL migration and eventual impact to a receptor, for example seepage to surface water. Composition-based risk is driven by toxic constituent presence within the LNAPL composition and risks posed by the chemical toxicity of components, say benzene a carcinogen, but also, of significant importance to the ILW case, the incorporation of radionuclides that may (complex and) partition into the LNAPL (Baker et al., 2003a,b; Chambers et al., 2004). Radionuclide partitioning to a buoyant, potentially mobile LNAPL hence raises the concern that radionuclides may migrate more rapidly to the surface (compared to advective or diffusive transport in groundwater) and circumvent attenuation opportunities otherwise afforded by transport solely in the aqueous phase such as greater timeframes for radioactive decay (Wealthall, 2002).

The vast majority of research and experience on LNAPL migration in the environment relates to contaminated land petroleum hydrocarbon fuel/oil LNAPL releases from storage tanks etc. (CL:AIRE, 2014; Kirkman et al., 2012; Mercer and Cohen, 1990). Whilst this research certainly holds relevance, the ILW-LNAPL scenario exhibits many distinguishing features. For example, the LNAPL source zone is purposely emplaced at considerable geological depth below the water table where conditions will certainly be anaerobic, its migration is intentionally inhibited by a multi-barrier disposal approach and upward vertical migration of LNAPL due to its buoyancy is key. Unusually, the LNAPL may be predominantly generated in situ within the waste packages as a result of degradation of organic materials, and the timeframes for radiological risk assessments are exceptionally long compared with those generally considered in the contaminated land application. These differences provide the rationale for ILW-specific LNAPL research within a GDF context.

Our research is centred around the UK's need to safely manage the disposal of its present ILW inventory totalling 265,000 tonnes (te) (NDA, 2010b) and contributes to the generic safety case for its disposal within a GDF (NDA, 2010c,d). The work forms a recent contribution to the on-going programme of research by the Nuclear Decommissioning Authority Radioactive Waste Management Directorate (NDA RWMD), now Radioactive Waste Management Limited (RWM), and its forerunner organisation, Nirex, to examine the impact on the safety case of the potential release of buoyant LNAPL from a GDF. As summarised by NDA (2012), the programme includes significant recent laboratory research and has examined, for example, discrete LNAPL generation potential within ILW, the role of complexants and partitioning to LNAPL, the influence of sorption and toxicity impact (Dawson and Magalhaes, 2012; Hunter et al., 2006; NDA, 2012). The goal of recent NDA-RWMD work undertaken by ourselves (and others) has been to develop and document a series of post-closure case safety arguments concerning LNAPLs in a GDF to support the generic proposition that the proposed type of disposal system will provide an appropriate level of safety (NDA, 2012; Watson et al., 2012).

Our goal, in preference to predicting LNAPL migration into the geological barrier from an assumed bulk source-term at the disposal vault–host rock interface, has been to examine ILW-LNAPL release potential starting from the individual waste package scale, its original source, and assess migration and transport within the disposal vault to the host rock interface. Aims were to determine whether the proposed deep geological disposal of ILW might lead to significant risk of LNAPL migration from waste packages and migration from a disposal vault and, to identify the features and processes within the system that most greatly affect the potential for LNAPL migration and transport. We present a summary of our underpinning ILW inventory and literature review to better define the nature of the ILW LNAPL

source term and numerical modelling to assess the likelihood of LNAPL release and subsequent migration from a waste package and the controlling processes. The reader is referred to Watson et al. (2012) (and appendices (*App.*)) for supporting detail and discussion of wider safety case arguments.

It is worthy of note at outset that a key control on the migration of LNAPL through the waste package and backfill system is the threshold displacement pressure at which LNAPL is able to enter initially water-saturated pores. Appropriate LNAPL displacement pressure data are uncertain and laboratory gas breakthrough pressures are often used to infer LNAPL pore entry (by accounting for differences in interfacial tension). Initial scoping calculations (Section 3.1) in which the LNAPL pore entry pressure was approximated using gas displacement pressure data for an ideal uniform pore structure resulted in almost all LNAPL being retained in the waste package. This is a useful and important result, and suggests that the rate at which LNAPL might be able to migrate from a waste package is likely to be small if the displacement pressure data is representative and if the integrity of the grout within the waste package and of the vault backfill is maintained. However given the uncertainty associated with the applicability of the measured gas displacement pressures, no credit has been taken for this resistance to migration in the scenarios that are otherwise considered herein. This is a conservative assumption and avoids one source of uncertainty in the modelling whilst allowing the effect on LNAPL migration (or resistance) of other features and processes in the system to be assessed. To ensure that the potential for LNAPL migration is not underestimated, we have made conservative estimates for all other parameters where there is significant uncertainty. This helps to facilitate the development of a comprehensive safety case based on multiple lines of reasoning.

2. Summary of Intermediate Level Waste LNAPL source zone nature

2.1. Intermediate Level Waste (ILW)

ILW is (www.nda.gov.uk glossary) "Waste with radioactivity levels exceeding the upper boundaries for Low Level Waste (LLW), but which do not need heating to be taken into account in the design of storage or disposal facilities. It arises mainly from the reprocessing of spent fuel, and from general operations and maintenance of radioactive plant. The major components of ILW are metals and organic materials, with smaller quantities of cement, graphite, glass and ceramics." This study is based on the 2007 estimate of 265,000 te for the total ILW inventory that will need to be disposed of in the UK. Some of the waste included in this inventory has not yet arisen, for example the inventory includes wastes from decommissioning of UK nuclear power station sites. This waste is, or will be, held in interim storage at ground surface and includes an estimated 8700 te of organic material (Pöyry, 2010). The UK proposes deep geological disposal of its ILW alongside, but separate from, high level waste (HLW) in a co-located GDF. ILW represents around 76% of the UK's radioactive waste volume requiring disposal, but only 2.5% of the radioactivity (NDA, 2010b).

LNAPLs are found in, or may be generated from, wastes containing organic materials present within the ILW/LLW (low level waste) part of the inventory. Our research on ILW-LNAPL composition and nature uses data from the Derived Inventory (DI) based on the UK's 2007 inventory (Pöyry, 2010). The Derived Inventory considers only wastes destined for deep geological disposal and is an enhancement of the National Inventory that includes information about how the waste will be immobilised and packaged and recognises some of the uncertainties associated with the information in the National Inventory. The DI subdivides organic material into: non-halogenated plastics, halogenated plastics, rubbers, organic ion exchange resins, cellulosic material, and other organic compounds (incl. hydrocarbon oils and laboratory chemicals) categories that are used in our analysis below and in the detail of Watson et al. (2012), *App. A.*

2.2. Waste package nature and geological disposal concept

The waste package (wasteform and waste container) serves as the first barrier to LNAPL migration. A range of standardised waste package types has been proposed, and used, for ILW. The majority of the waste that has the potential to be associated with LNAPLs has been or will be packaged in 500 litre (L) vented stainless steel containers using the one of the following types of wasteforms (in order of probable increasing effectiveness of LNAPL containment):

- *Annular grouted* — an annulus of cementitious grout surrounds the waste, which comprises 200 L carbon steel waste drums super-compacted to form pucks (Fig. 1). Containment of LNAPL after closure of a GDF may be reduced if cracks develop in the grout annulus and/or if corrosion of the container were to allow flow through the waste package. Much of the inventory of plastics, rubbers and other possible LNAPL precursors is expected to be associated with this wasteform.

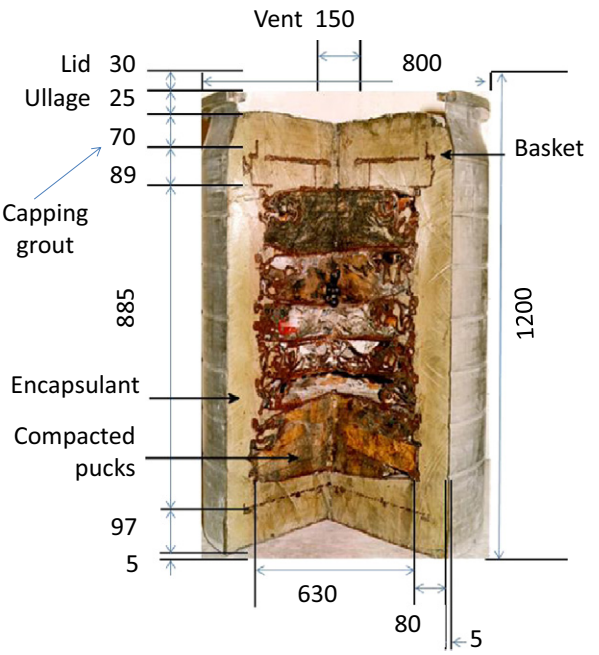

Fig. 1. Photograph of a cut-away 500 L annular-grouted simulated waste package containing ILW stimulant with dimensions (mm) shown as used in model simulations (photograph supplied by NDA).

- *In-container grouted* — solid wastes within a waste container are surrounded and infiltrated by grout that may perhaps react with and immobilise any LNAPLs present. The wasteform is potentially less prone to crack development facilitating migration of the entire package LNAPL inventory than the annular grouted example. Wastes may consist of relatively large items (e.g. size-reduced mechanical components) that could contain traces of oil, solvent or grease as well as smaller items (e.g., shredded plastic).
- *In-drum mixed wasteform* — grout is mixed intimately with the waste (often a sludge) within the waste container and is likely to completely encapsulate any LNAPLs in the waste at the grain scale. The wasteform does not contain interfaces at which cracks are likely to originate. Any oils, solvents and greases present are likely to be dispersed throughout the package.

The work reported herein considered RWMD's illustrative example disposal concept for ILW in a higher strength host rock (NDA, 2010c,d). Waste packages would be placed in large engineered vaults, c. 650 m below ground surface, with a cross section of c. 16 m by 16 m and a length of c. 300 m. Waste packages would be stacked in 7 layers, leaving a c. 6 m gap between the uppermost package of the resulting waste stack and roof of the vault. The waste packages would be surrounded by a cementitious backfill. An engineered vault lining may also be present that could impede LNAPL migration from the near field to the geosphere.

LNAPL migration from a waste package requires a pathway from the LNAPL source location to the outside of the package. In this context it is important to recognise that most ILW waste packages are vented and hence fractures connecting the LNAPL source region to the vent may provide an initial pathway. Container corrosion and degradation of the grout, with time, may create additional pathways through the waste package. These pathways may be advective if a head gradient is present. If free gas is present in the waste package, any migrating LNAPL likely accumulates at the top of the water-saturated region, unable to move from the waste package until gas saturations decline to residual values. Resaturation of the waste package by water is expected to be relatively fast (years to decades) for a higher strength host rock. The ullage space (Fig. 1) may represent an important capillary break preventing LNAPL capillary-facilitated entry into the backfill. There is a fundamental driving force requirement to move LNAPL out of the waste package as a free phase (as opposed to dissolved-phase). Options include: sufficient agglomeration of LNAPL for its buoyancy to exceed the displacement pressure for migration through grout/backfill; capillary forces in the grout or overlying unsaturated region are sufficient to draw LNAPL out of the source region; waste package pressurisation due to unexpected vent blockage forcing fluids out of the waste package and advection if a connected pathway forms through the package. LNAPL migration requires degradation and dissolution timescales to exceed times required for LNAPL movement from the waste package.

2.3. Sources of LNAPL within Intermediate Level Waste

'As-disposed' LNAPL originally present within the ILW is not expected to result in the migration of a free LNAPL phase from the waste package. Waste forms are designed to provide effective immobilisation of this component of the LNAPL inventory by encapsulation (Section 2.2), and the compliance process limits the volumetric LNAPL content of waste packages. The most probable DI category accounting for this wastestream is 'other organic compounds' (incl. hydrocarbon oils and laboratory chemicals). Supporting experimental work (summarised by NDA, 2012), has shown that: LNAPL loadings of 4–8% by weight do not adversely affect wasteform properties including setting; LNAPL immobilisation is enhanced by the presence of solid precipitates, especially magnesium hydroxide; and, decade-long experiments on Nucleol 520 oil encapsulated in grout suggests the wasteform is robust (Craven, 2005). Any non-encapsulated LNAPL is still likely dispersed and immobile throughout the wasteform and will remain so unless residual saturations are exceeded that are typically c. 20% for porous media (Mercer and Cohen, 1990). These are around an order of magnitude greater than expected waste package maximum loadings. Very gradual decline of the isolated immobile LNAPL due to diffusive–dissolution transfer to the aqueous phase, possibly with (bio)degradation mass removal, is the expected long-term fate of as-disposed LNAPL; a buoyant LNAPL release is not anticipated.

'Secondary' LNAPL may be generated in-situ within the various waste package types from precursor organic material originally present within the ILW. The organic material categories – non-halogenated plastics, halogenated plastics, rubbers, organic ion exchange resins, cellulosic material – have varying potential to generate LNAPL which we have assessed in relation to the ILW DI in *App. A* of Watson et al. (2012), drawing upon the process-based research summarised by NDA (2012) and summarised further below for PVC (polyvinyl chloride). Secondary LNAPL generated from degradation of, and the release of, additives from (mainly) plastics will typically not be immobilised as effectively as 'as-disposed' LNAPL since the LNAPL is not mixed with the grout at the time of wasteform manufacture. Annular grouted waste packages (Fig. 1) are expected to provide the most concentrated mass of organic precursor material (in the compressed waste pucks), the least containment and the largest inventory of LNAPL per package of the three generic waste package types.

Chemicals, some with potential to form a LNAPL, may be released from organic plastic materials due to chemical-, radiolytic- and or thermal-induced degradation leading to potential disintegration of the polymer structure. Release of additives within plastics such as plasticisers that are not chemically bound to the polymer is more likely to occur without degradation. This is due to their molecular structure allowing the chemical to be radiation tolerant (although not necessarily immune); for example, the delocalised aromatic ring of phthalate plasticisers may dissipate radiolytic energy without molecular breakdown. The overall degrading polymer structure combined with thermal stress on a material that will increase plasticiser-additive diffusion rates may lead to the accumulation of chemical at the plastic interface and potential coalescence to a LNAPL. Such a thermally induced effect may be observed, for example, in aged electrical wiring where a sticky, oily brown film of LNAPL phthalate plasticiser may accumulate around the increasingly brittle wire-insulation material. Although phthalates are judged the most persistent, potential LNAPL-forming chemical type in plastic materials, they are

nevertheless susceptible to degradation (e.g. alkaline hydrolysis (Section 2.4)), under the alkaline conditions of the wasteform grout and surrounding backfill and in the presence of ionising radiation.

2.4. PVC (polyvinyl chloride) plastic: secondary LNAPL generation and additive fate

The expected behaviour of PVC is reviewed in detail, by way of example, but also because of its significance to the ILW LNAPL source term. The reader is referred to NDA (2012) which provides a comprehensive summary of the experimental and theoretical work that has been carried out to estimate the amounts and compositions of LNAPLs that might be generated from the various precursor materials in the inventory; and, our own work in Watson et al. (2012) *App. A, B*, where we detail further the LNAPL chemicals that might potentially be generated from the various organic precursor material categories that serve as the basis for our LNAPL source term (Section 2.5). LNAPL generation is predicted to be most significant from the halogenated plastics, in particular the phthalate plasticisers found in flexible polyvinyl chloride (PVC) plastics. Additives, such as plasticisers and fillers are used to tailor PVC for a variety of applications, such as flexible yet strong plastic bags. Amounts of plasticisers present vary significantly across products and manufacturers, but typically comprise 30–50% of the PVC (Smith et al., 2010) with greater contents generally in more flexible material products. In the DI, PVC is typically found in the form of a semi-flexible cable insulator or plastic bags (Dawson and Magalhaes, 2012). Pöyry (2010) estimates the total mass of ILW halogenated plastics to be between 3110 te and 3681 te with a best estimate of 3498 te. Of this, PVC is estimated to comprise 80–95% of the wastestream.

LNAPL production from thermal ageing has been investigated for flexible PVC films in de-ionised water and alkali solutions (Dawson, 2012; NDA, 2012). Fig. 2 shows an oily (NAPL) viscous residue observed in that work from PVC after 60 d at 80 °C in pH 12 $Ca(OH)_2$ solution. The composition of the oily residue could not be analysed successfully, nor could the density of the residue NAPL be determined. A buoyant LNAPL was not obvious at the water–solution surface; however, we speculate this could be due to the adherence of the viscous oily NAPL to the PVC. After 120 d, a PVC mass loss of ~30% was determined and phenolic compounds were detected in solution. However, oily residues were not observed under neutral conditions at 80 °C or after gamma irradiation to 150 kGy and 10 MGy at room temperature under alkaline conditions (Dawson, 2012; NDA, 2012).

In terms of aqueous-phase solution contents, Reed and Molecke (1993) have observed that various generic degradation products were released when PVC was irradiated to 120 kGy, with water-soluble acetone most abundant (~50%) and not expected to lead to LNAPL formation. Total organic carbon (TOC) in solution has also been observed to increase by 10 to 60 times following irradiation compared to non-irradiated control PVC samples (Dawson, 2012; NDA, 2012). Declines in pH are observed in irradiated solutions as general radiolysis mechanisms of PVC polymer disintegration will yield hydrogen chloride (Dawson and Magalhaes, 2012). Solution contents could perhaps include degraded additive and particularly degraded polymer contributions, including soluble alcohols, aldehydes, ketones and carboxylic acids. Common PVC plasticisers include high molecular mass phthalates such as diisononyl phthalate (DINP), diethyl hexyl phthalate (DEHP), dioctyl phthalate (DOP) and diisodecyl phthalate, which have low aqueous solubilities (<0.5 mg/L). These phthalates are hence unlikely to have very significant aqueous-phase concentrations, but have potential to form a

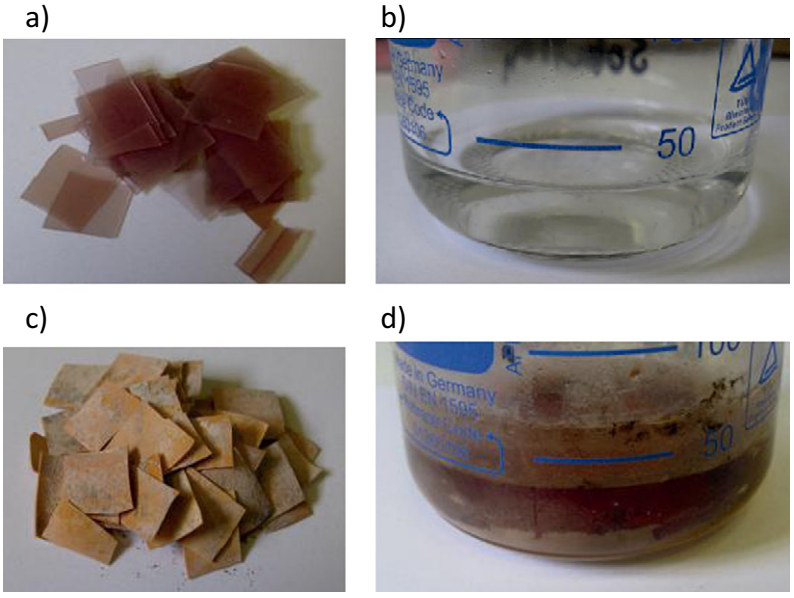

Fig. 2. Laboratory experiments comparing PVC (Weston Vinyls) films and corresponding aqueous solutions after leaching for 60 d at 80 °C in: (a, b) de-ionised water; and, (c, d) alkali $Ca(OH)_2$ solution at pH ~ 12. Only the alkali case shows significant change in appearance and mass loss from the films and the accumulation of oily viscous residues in solution.
After NDA (2012).

LNAPL film if fluxes from the internal plastic to its interface exceed dissolution fluxes away from that interface into aqueous-phase solution. Abiotic (hydrolysis) and biotic reactions may occur for phthalates in the aqueous phase to some degree depending on conditions; if significant, these may enhance LNAPL dissolution fluxes due to the increased chemical concentration gradients induced thereby lowering the potential for LNAPL accumulation.

Under dry conditions (potentially relevant until a waste package becomes water-saturated), experience shows that where PVC has been irradiated to high doses (>1 MGy, albeit not quantified), a sticky plasticiser residue is observed on PVC cable components indicating that the plasticisers are mobile and radiation tolerant (Dawson and Magalhaes, 2012). In air and nitrogen gas, when irradiated to 150 kGy and 10 MGy, plasticisers were released from PVC as evidenced by a waxy appearance (Dawson, 2012; NDA, 2012). For (dry) PVC cable material that has been aged and maintained at 70–110 °C, there is a reported weight loss of 17% due to plasticiser loss (Dawson and Schneider, 2002). Comparing wet and dry experiments suggests that it is possible that under some conditions small amounts of plasticiser may diffuse out of the polymer into the solution but then degrade further under irradiation, or form a solution in the aqueous phase (Dawson, 2012; NDA, 2012). Therefore, the net LNAPL production may be dependent on a balance between the rates of diffusion and degradation in the period, expected to be c. 100 y, between waste packaging and backfilling of a GDF and the rate of degradation once any LNAPL that has been generated comes into contact with alkaline porewater following resaturation of the waste package. The expected temperature increase associated with GDF backfilling will increase the diffusion rate of any plasticisers remaining within the matrix (Dawson, 2012; NDA, 2012).

Considering phthalate fate within the aqueous phase, although high molecular mass phthalates released from PVC and other plastics are notably persistent in the water environment globally, they do have some degradation potential (Liang et al., 2008) that may, even at low rates, become significant over GDF timeframes. Hydrolysis of phthalate esters is favoured under the alkali conditions associated with cementitious backfill. Schwarzenbach et al. (1993), drawing on the studies of Wolfe et al. (1980a,b) that cover phthalates ranging from dimethylphthalate (DMP) up to diethyl-hexyl-phthalate (DEHP), confirm the importance of base-catalysed phthalate hydrolysis at high pH with significantly reduced rates at neutral and acidic pH. Also, second order base-catalysed rate constants markedly decrease with increased molecular mass, for example, from 6.9×10^{-2} M^{-1} s^{-1} for DMP (dimethylphthalate) to just 1.1×10^{-4} M^{-1} s^{-1} for DEHP (at 30 °C) (Schwarzenbach et al., 1993). DEHP is of comparable molecular mass and potentially similar reactivity to phthalates such as DOP and DINP. Hence these high molecular weight phthalates may be expected to exhibit some persistence, even under high pH conditions that favour hydrolysis.

Some biotic contributions may be anticipated to enhance phthalate degradation (Jonsson et al., 2006; Liang et al., 2008). However, high temperature, high bulk pH (~12) and perhaps low water conditions are likely to restrict microbial degradation to favourable environmental niches (Askarieh et al., 2000; Humphreys et al., 2010). pH 11.5 is believed to be the highest pH reported for bacterial growth with optimal growth of alkaliphiles at pH 9–10 (Sorokin et al., 2012). To provide context in terms of the chemical environment within the near field of a GDF in the UK context (NDA, 2010e): the Nirex Reference Vault Backfill (NRVB) provides a high pH environment of pH 12.5, buffered by portlandite, for several hundred thousand years falling to around pH 10, buffered by calcium silicon hydrate, for more than a million years (dependent on groundwater flow rate and composition).

2.5. LNAPL source term

As the LNAPL source term associated with ILW disposed of in a GDF may be primarily based upon secondary LNAPL generated in situ that is shown to be inherently complex (as illustrated for PVC), it is unsurprising that defining a representative ILW LNAPL source term, at any scale, is non-trivial. Laboratory observations of actual LNAPL release from the range of plastics associated with ILW, such as the oily phase observed for PVC in Fig. 2, have proven rare (NDA, 2012) (and is the subject of on-going RWM research). In order to be conservative, however, the ILW source-term was assumed to include any released chemical that has a potential to exist as a LNAPL by virtue of its physical–chemical properties. It was also assumed that at the waste package scale, secondary LNAPL formed may be sufficiently local to agglomerate (coalesce) to from a continuous LNAPL body that may be able to migrate. This is again a conservative assumption for which further supporting data would be beneficial; for example, this could include observational data from the characterisation of decades-old waste packages.

Our approach to defining a source term has been to estimate a 'LNAPL mass potentially generated' ($Lm_{potential}$) from the ILW inventory that was based on our analysis of the DI (Pöyry, 2010). Fig. 3 compares our $Lm_{potential}$ estimate with the ILW mass of organic material to be disposed to the UK's GDF subdivided to the various organic material ILW categories. *The* $Lm_{potential}$ for most ILW DI organic material categories equates to the secondary LNAPL mass potentially generated. This typically equates to the mass of additives, usually plasticisers, present in the precursor organic material (plastic) that are judged sufficiently mobile to release from the (degraded) polymer, and are also sufficiently radiation tolerant to allow persistence to form a LNAPL. The assumptions underpinning these judgments are outlined in Dawson and Magalhaes (2012) and in our detailed application of those assumptions to the DI and our estimation of $Lm_{potential}$ (Watson et al., 2012, *App. A*). For the 'other organic compounds' category, $Lm_{potential}$ was equated to the as-disposed LNAPL mass. It is emphasised that no credit is taken for prior encapsulation of mass or subsequent degradation of LNAPL mass via abiotic or biotic reactions. $Lm_{potential}$ is judged a maximum potential mass; it is regarded as an upper bound and over-estimate of the likely LNAPL source-term mass. It is noted that extrapolation of some of the experimental observations discussed in Section 2.4 (Watson et al. (2012), *App. A*) would give much lower masses (for example, the gamma irradiation results of Dawson (2012)).

Fig. 3 indicates an overall $Lm_{potential}$ upper bound value of 1300 te of LNAPL of which halogenated plastics, mostly PVC, account for 740 te. It is entirely reasonable to exclude the 'other organic chemicals' from the total LNAPL as these will almost all be encapsulated and or very dispersed and immobile. This

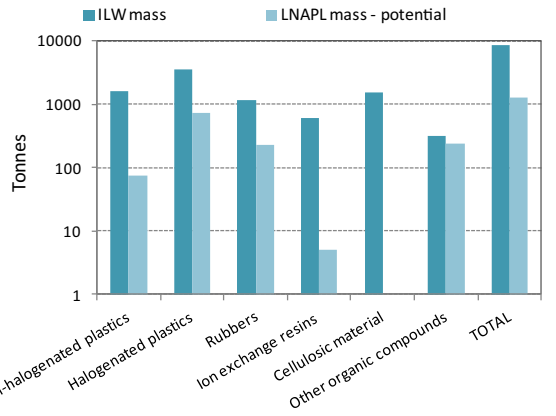

Fig. 3. Comparison of inventory ILW mass to be disposed in the UK's GDF with LNAPL mass–potentially generated ($Lm_{potential}$) for the various organic material categories (see Watson et al., 2012 for underpinning data for specific plastics etc. contributing to the various categories).

would yield an $Lm_{potential}$ of just over 1000 te that is still regarded as a pessimistic estimate as degradation of, or incomplete release of additive plasticiser is not considered and is a significant probable contribution to diminishment of the accumulated mass over time.

In order that our numerical modelling predictions are appropriate to a safety case, definition of the source term for our modelling work at the waste package scale has adopted a similar conservative approach. We use inventory data for a wastestream known to be rich in organic material and apply similar assumptions to those outlined above for the estimation of $Lm_{potential}$ that allows an upper bound estimate of LNAPL to be generated. Additionally, we allow some variation of secondary LNAPL generated within the simulated scenarios simulated to examine source term sensitivity to LNAPL composition (see later Table 1). It is recognised that, in reality, the source term will be time-dependent, governed by the timescales of in situ secondary LNAPL generation, but determination of appropriate timescales is beyond the scope of this work. Our modelling therefore conservatively assumes that the entire source term is available at the time of emplacement.

The $Lm_{potential}$ estimate represents 18% of the total mass of organic pre-cursor material (excluding cellulose) in the ILW inventory. Being conservative, it suggests that at least 82% of the ILW organic precursor material either remains as a 'solid' polymer plastic or would be transferred to the aqueous phase. This could hence represent a considerable organic loading locally to the aqueous phase that may influence LNAPL behaviour, for example, via: their aqueous-phase presence modifying LNAPL dissolution; indirectly through consumption of electron acceptors in biodegradation reactions that may have otherwise been used in the biodegradation of LNAPL (dissolved) chemical; their degradation inducing changes in pH and redox conditions; and, directly through acting as an electron donor in biodegradation reactions where the LNAPL chemical is acting as an electron acceptor, in say dechlorination reactions (Watson et al., 2012, *App. B*). Literature associated with high organic content landfill leachate would hold some analogous relevance (Christensen et al., 2000).

Table 1
LNAPL mass estimates for a 500 L waste package used in the source term modelling for the various simulation scenarios developed from the 2D03 inventory. After Watson et al. (2012), *App. C*.

Waste category	2D03 inventory mass kg	Scenario 1 Phthalate-rich 2D03 LNAPL kg	Scenario 2 Central 2D03 LNAPL kg	Scenario 3 Maximum 2D03 LNAPL kg
PVC	126.48	31.62	31.62	63.24
Rubber	52.08	7.29	7.29	10.42
Polythene	29.76	0	0	4.46
Cellulose	29.76	0	0	0
Other organics	11.16/22.32[a]	0	8.48	16.96
Total LNAPL		38.91	47.39	95.08
% LNAPL		16%	19%	37%

[a] Assumed as 1.5% of the inventory for Scenario 2 and 3% for Scenario 3.

2.6. LNAPL composition: density and viscosity

It is not only the mass of LNAPL potentially present that is significant, but also its composition. Composition may significantly impact the intrinsic properties of the LNAPL, for example its density, viscosity and solubility, which, in turn, influence the fate and migration of a LNAPL, for example, respectively, its buoyancy, its migration rate and dissolution (and depletion) into the aqueous phase. Clearly, with ILW being composed of many different wastestreams derived from different processes as well as the consideration that generation of secondary LNAPL, a complex heterogeneous process, is involved, it is to be expected that composition is likely heterogeneous within and between both wastestreams and individual waste packages within a wastestream. That said, the secondary LNAPLs generated are anticipated to be dominated by plasticiser additives, particularly those that are more radiation tolerant such as the phthalate chemicals (Section 2.3) (Watson et al., 2012).

Fig. 4 serves as an indicator of relative NAPL mobility, and plots literature pure-phase chemical viscosity (log) versus density for a wide range of organic liquid chemicals. The figure plots not only LNAPL chemicals, but also some dense non-aqueous phase liquids (DNAPLs) that have a density greater than water as well as some compounds that may be miscible (form a single phase) with water, for example methanol. The majority of chemicals plotted are mentioned as either plastic composition precursors or decomposition products detected in the laboratory studies and literature we have reviewed targeting the fate of ILW organic material categories (Watson et al., 2012, *App. A, B*; NDA, 2012 and therein). Various n-alkane and common fuel/oil hydrocarbons have also been added to the plot for convenient reference, some of which may be within the ILW 'Other Chemicals' category. The phthalates predominantly mentioned in the reviewed plastics literature, for example for PVC, tend to be the higher molecular mass phthalates that are very viscous and 'just' an LNAPL of weak density contrast (c. 0.98) compared to a water density in the GDF environment estimated (and modelled) at 1.02. They are hence of very weak buoyancy contrast. High molecular mass phthalate rich LNAPLs would hence be just buoyant and migrate very slowly upward

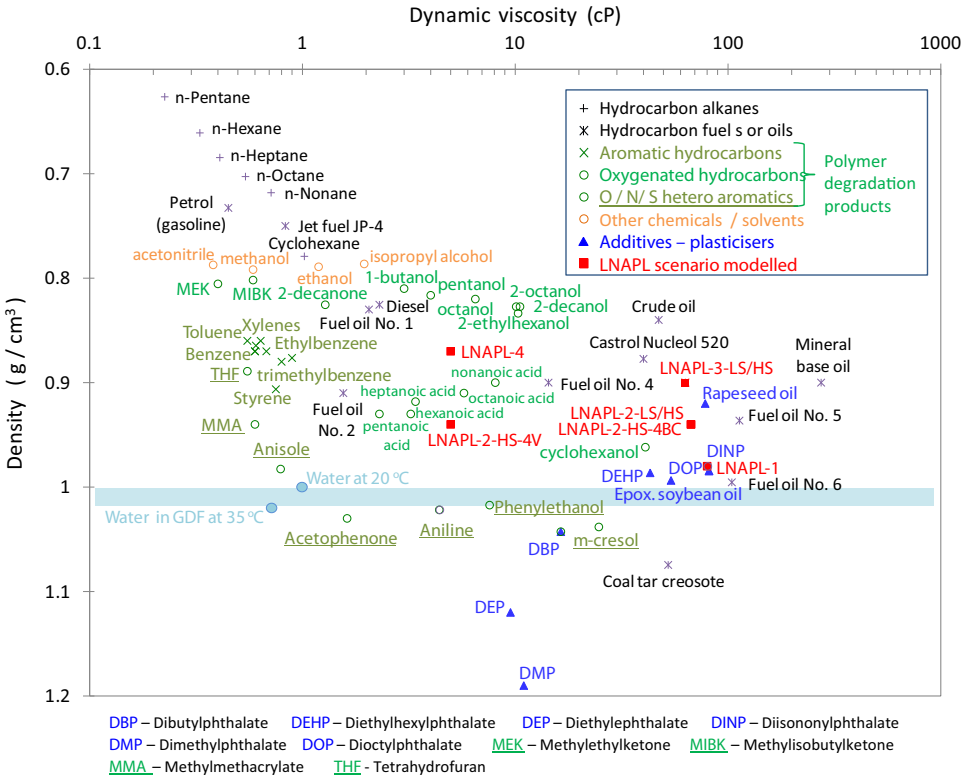

Fig. 4. Plot of NAPL density versus NAPL dynamic viscosity for chemicals associated with ILW that could form or partition into a NAPL. Chemicals are colour-coded to additives (plasticisers) (polymer degradation products could arise from additives too), other organic compounds and other reference chemicals such as hydrocarbon fuels/oils that could occur in wastes or simply provide context. The four LNAPL scenario variants are also shown. Parameter values are based on literature tables typically quoted at 20–25 °C, example sources include: Mercer and Cohen (1990), Montgomery (2007), Newell et al. (1995) and Schwarzenbach et al. (1993). Reference points for water are plotted for de-ionised water at 20 °C (1 g cm^{-3}, 1 cP) and an anticipated GDF water quality at 35 °C of density 1.02 g cm^{-3} (1020 kg m^{-3}) and viscosity 0.72 cP (7.2×10^{-4} Pa s) used in the numerical modelling that were based on expected groundwater inorganic compositions for a typical host rock environment.

due to their elevated viscosity assuming they are able to overcome pore entry pressures. Their behaviour would be inversely comparable to the very gradual penetration to depth below the water table of surface releases of coal tar–creosote (plotted in Fig. 4) DNAPLs of comparable viscosity and weak density contrast (density c. 1.05) (Gerhard et al., 2007). An increased proportion of the lower molecular weight, but denser phthalates (Fig. 4) would lead to a neutral to dense (D)NAPL scenario thereby removing the buoyancy hazard in the GDF context. Their solubility is, however, greater and their preferential dissolution may lead to this being a temporary decreasing DNAPL influence.

Although many of the polymer degradation products are potentially more buoyant and mobile due to their lower viscosities and densities (Fig. 4), they are much more soluble than the additives (Watson et al. 2012, *App. B*). Hence on the timescales of interest to a GDF scenario, their depletion from the LNAPL may become significant and occur relatively quickly leaving an increasingly additive/phthalate-enriched LNAPL with time. Some of the specifically mentioned Other Chemicals in the ILW wastestreams were miscible (high solubility) laboratory solvents and if incorporated within a multi-component LNAPL mixture they would be expected to likewise deplete rapidly and accordingly reduce LNAPL density contrast and buoyancy.

2.7. LNAPL source scenarios simulated

Our waste package simulation scenarios were based on the plutonium-contaminated materials (PCM) wastestream 2D03 (Watson et al., 2012, *App. C*). This specific wastestream was selected, not only to provide realism to the modelling, but also because it exhibited the following: a high potential inventory of LNAPL — it contained significant PVC with diverse organic material categories present; potential for LNAPL generated from the waste to agglomerate and become potentially mobile — it is packaged using an annular grouted wasteform and hence concentrated pucks of organic material are present and there is potential for organic material mobility and coalescence; and to be present in sufficient numbers that the LNAPL generated might be significant on a GDF scale — over 10,000 waste packages have been produced. Soft PCM wastes from the 2D03 wastestream are currently placed in 200 L carbon steel drums, which are super-compacted to form the pucks as illustrated in Fig. 1.

The derivation of the LNAPL inventory per waste package was based on the wastestream datasheet (NDA, 2007) and estimates of secondary LNAPL yields corresponding to our upper-bound estimate, $Lm_{potential}$. A typical 2D03 wastestream comprises (by weight): PVC 17%; rubber 7%; cellulose 4%; polythene 4%; other organics up to 3%; steel (drums) 62%; and rubble/soil/glass 3%. The LNAPL composition for the 2D03

wastestream is expected to be dominated by the radiation-tolerant high molecular mass phthalates, for example, DINP, DEHP/DOP. Of the ILW wastestreams, 2D03 is judged one of the most likely to have the potential to generate significant quantities of buoyant LNAPL.

Making various conservative assumptions, three LNAPL mass-composition scenarios were proposed for model simulation. These were: Scenario 1, 'Phthalate-rich 2D03 LNAPL'; Scenario 2, 'Central 2D03 LNAPL'; and, Scenario 3, 'Maximum 2D03 LNAPL'. The variations are a result of assuming that the 'other chemicals' category do (Scenario 2), or do not (Scenario 1), contribute to the LNAPL mass; either is realistically valid with arguably Scenario 1 being the most realistic and common. Scenario 3 is a more pessimistic alternative that invokes upper-bound estimates of LNAPL that could be released from each of the organic material precursor categories. It is viewed as the least plausible scenario for 2D03 and hence most conservative in that the LNAPL mass is maximised. Table 1 quantifies the contributions of the organic material categories to the various 2D03 LNAPL mass estimates used in the source term modelling.

A further Scenario 4 'Low viscosity LNAPL' is simulated that, although judged unrealistic, allows the sensitivity to a higher density contrast, lower viscosity LNAPL to be assessed. Properties are not based on the 2D03 wastestream, rather a synthesised combination of hydrocarbon oil used by the nuclear industry (Castrol Nucleol 520 lubricating oil) and a typical LNAPL encountered at petroleum contaminated-land sites with both low density and low viscosity and hence high mobility. Our review, including Watson et al. (2012) and the supporting literature (NDA, 2012) do not support that such an LNAPL is viable in significant volumes in the GDF-ILW context. Properties of all the Scenario LNAPLs are detailed in Table 2 with further justification of value selection given by Watson et al. (2012), *App. C*. Overall, the range in properties permitted simulations to be conducted that gave the benefit of sensitivity testing across a range of LNAPL types recognising the uncertainty in ILW LNAPL composition and quantities. The four LNAPL scenarios are marked on the Fig. 4 viscosity–density plot to provide an indication of the relative mobility of the LNAPLs simulated.

3. Modelling approach

This section describes the models that have been developed to assess whether LNAPLs might be able to migrate out of a waste package into the surrounding backfill. It starts from the assumption that the pessimistic upper bound inventory of LNAPLs might be present in those packages that contain LNAPL precursors.

3.1. Model approach

Consistent with the overall ambition to better understand the nature of any source term of LNAPL emanating from a GDF, the aim of the numerical modelling is to first understand the potential for LNAPL to migrate from the waste package in which it (or its precursor material) is initially present (Fig. 1), and then to determine likely timescales for migration through the overlying backfill before the LNAPL is able to enter the host rock. This is consistent with the "multi-barrier" approach to the engineering design of a GDF and allows the efficacy of each of the engineered barrier system to be investigated. The models comprise a single waste package in isolation; no interference from LNAPLs released from neighbouring packages is considered. Scenarios considered the waste package to either be: intact (as emplaced); contain cracks in the grout; or include an annular failure in the waste package (e.g. due to corrosion at a weld) and/or cracks in the encapsulant. In the latter case, the annular failure was assumed to be located at the bottom of the waste package to maximise the pressure gradient through the waste package (given the boundary conditions that have been chosen; see Section 3.4.2) and therefore maximise the potential for migration of LNAPL out of the package. Since the rate of LNAPL generation from precursor material is uncertain, the total potential package LNAPL inventory is assumed to be available at the start of the modelled period.

Where possible, realistic assumptions on LNAPL and media properties have been made and where data are missing or uncertain, conservative assumptions have been made so that timescales for migration are not overestimated. In particular degradation of LNAPL is not included in the models, since realistic rates of LNAPL degradation under in situ conditions are uncertain, and the closest package to the vault roof has been chosen in order to provide the shortest buoyant pathway to the host rock.

No direct effects of the choice of host rock have been taken into consideration in the modelling, although the NRVB backfill that is assumed is currently only envisaged for use in higher strength host rocks (NDA, 2010d). The backfill dimensions are consistent with this choice. Models extend only as far as the top of the backfill in the vault. Differing rates of resaturation in different host rocks would affect the time at which LNAPLs can start to migrate from the waste package. The modelling presented here has as its starting point the time at which the waste package fully resaturates with water, meaning that residual gas saturations are reduced to a minimum (it is assumed in the modelling that there is insufficient gas in the waste package to significantly affect the LNAPL migration). This is expected to be rapid for higher strength host rocks,

Table 2
Physical properties assumed for the various Scenario LNAPLs simulated that are largely based on weighted average of their key component chemicals; for example phthalate additives are based on the mean of DOP and DINP (for further rationale, see Watson et al. (2012), *App. C*).

	Scenario 1	Scenario 2	Scenario 3	Scenario 4
	Phthalate-rich 2D03 LNAPL	Central 2D03 LNAPL	Maximum 2D03 LNAPL	Low viscosity LNAPL
LNAPL mass in waste package (kg)	38.9	47.4	95.1	47.4
Molar mass (g/mol)	405	255	303	226
Density (g/mL)	0.98	0.94	0.90	0.87
Viscosity (cP)	80	67	63	5
Aqueous solubility (mg/L)	0.3	89[a]	61[a]	100

[a] Initial effective solubility based on Raoult's law analogue that will significantly decline over time.

and so in the models it is assumed that the mobile LNAPL phase is still located in the pucks at the start of the simulation.

3.2. Numerical model

All simulations were performed using Quintessa's general-purpose modelling code, QPAC (Quintessa, 2012) and its associated multiphase flow (MPF) module. QPAC includes a variable time-step, variable order backward difference formula Differential Algebraic Equation (DAE) solver to solve a system of discretised partial differential and algebraic equations. The MPF module implements Darcy's equations for immiscible multiphase flow, coupled with transport of dissolved species using the following set of equations:

$$S_w + \Sigma_j S_j = 1 \tag{1a}$$

$$p_{c_j} = p_j - p_w \qquad j = 1, \ldots, N_f \tag{1b}$$

$$\frac{\partial}{\partial t}(\theta \rho_w S_w) = -\nabla \cdot (\rho_w u_w) \tag{1c}$$

$$\frac{\partial}{\partial t}\left(\theta \rho_j S_j\right) = -\nabla \cdot \left(\rho_j u_j\right) - R_j^{\text{diss}} \qquad j = 1, \ldots, N_f \tag{1d}$$

$$\frac{\partial}{\partial t}\left(\theta \rho_w S_w c_j\right) = -\nabla \cdot \left(c_j \rho_w \boldsymbol{u}_w\right) + \nabla \cdot \left(D_j \nabla c_j \rho_w\right) + R_j^{\text{diss}} \qquad j = 1, \ldots, N_f \tag{1e}$$

$$\theta = \theta_0 e^{\beta(p - p_0)/\theta_0}. \tag{1f}$$

Here subscript w represents the water (wetting phase) fluid and subscripts $j = 1, \ldots, N_f$ represent N_f co-existing fluids. S_i (−) is the saturation of each fluid, p_i (Pa) is its pressure, ρ_i (kg/m^3) is its density and $\boldsymbol{u}_i$ (m/s) is its Darcy velocity; p_{c_j} (Pa) is the capillary pressure across the interface between the jth co-existing fluid and water; c_j (kg/kg) is the dissolved concentration of the jth co-existing fluid in the water, D_j (m^2/s) is its effective diffusion coefficient in water and R_j (kg m^{-3} s^{-1}) is its rate of dissolution. θ (−) is the porosity of the medium, with θ_0 (−) its porosity at reference pressure p_0 (Pa), and β (Pa^{-1}) is its compressibility.

The set of Eqs. (1a)–(1f) consists of $3N_f + 3$ equations for the unknown saturations and pressures of each fluid (wetting and non-wetting), the dissolved concentration of each non-wetting fluid and the porosity. In the modelling described here only a single non-wetting LNAPL phase is simulated, so $N_f = 1$. The subscript n will therefore be used subsequently to denote properties of the LNAPL.

The Darcy velocity u_i is given by

$$u_i = -\frac{k_i}{\mu_i}\nabla(p_i + \rho_i g z), \tag{2}$$

where μ_i is the fluid viscosity (Pa s), g (m/s^2) is the acceleration due to gravity, and z (m) is the vertical coordinate (positive upwards). k_i (m^2) is the saturation-dependent permeability of the medium to fluid i, which is expressed in terms of the intrinsic permeability k (m^2) of the medium and the relative permeability k_i^{rel} (−) of the medium with respect to fluid i as

$$k_i = k_i^{\text{rel}}(S_i)k. \tag{3}$$

The hydraulic parameterisation of the grout and backfill materials in the model assumes a porous media parameterisation and follows the Brooks and Corey (1964) convention, in which the capillary pressure and relative permeability curves are expressed in terms of the effective water and LNAPL saturations, S_{we} (−) and S_{ne} (−), which are given by

$$S_{we} = \frac{S_w - S_m}{1 - S_m}, \text{ and} \tag{4a}$$

$$S_{ne} = \frac{S_n}{1 - S_m}. \tag{4b}$$

S_m (−) is the residual aqueous phase saturation. The capillary pressure between the water and LNAPL phase is defined in terms of displacement pressure as

$$p_{c_n} = \frac{p_{nd}}{S_{we}^{1/m}}, \tag{5}$$

where p_{nd} is the LNAPL–water displacement pressure (Pa) and m (−) is the pore size distribution index.

Relative permeability curves for water and LNAPL in the grout and backfill are given by

$$k_w^{\text{rel}} = S_{we}^{(2+3m)/m}, \text{ and} \tag{6a}$$

$$k_n^{\text{rel}} = S_{ne}^2\left(1 - S_{we}^{(2+m)/m}\right) \tag{6b}$$

respectively.

The waste pucks are assumed to behave like a fractured media, as opposed to the porous media treatment for the grout and backfill, with their relative permeability assumed to be simply proportional to saturation, so that $k_w^{\text{rel}} = S_w$ and $k_n^{\text{rel}} = S_n$. If any fractures are present in the model (i.e., in the failed package scenarios) then these are treated in the same way. These choices result in large relative permeabilities in the media that are represented as fractured and ensure that the potential for a LNAPL pathway is not underestimated. The permeability of the ullage space in all models is simulated assuming no dependence of the net permeability on saturation, so that $k_w^{\text{rel}} = k_n^{\text{rel}} = 1$. The capillary pressure in the waste pucks, ullage and any fractures is taken to be $p_{c_n} = 0$ Pa.

The effective diffusion coefficient of dissolved LNAPL is modelled as a function of the material porosity and tortuosity using a simple linear Archie's law assumption,

$$D_n = \theta \tau D_{n,pore}(T) \tag{7}$$

where τ (−) is the tortuosity and $D_{n,pore}$ (m^2/s) is the diffusion coefficient in water at temperature T (K), which depends on

the molar volume of the LNAPL and is modelled using the Wilke–Chang equation (Wilke and Chang, 1955),

$$D_{n,pore} = 7.4 \times 10^{-8} \sqrt{\psi_w M_w} \frac{T}{\mu_w V_{Nb}^{0.6}}. \quad (8)$$

Here ψ_w (−) is an association parameter (which is taken to be 1 for non-associated solvents and 2.6 for water), M_w (g/mol) is the molecular weight of water, T (K) is the temperature and V_{Nb} (cc/mol) is the LNAPL molar volume at its normal boiling point. Since all solvent terms in the Wilke–Chang equation will be common for all LNAPLs, only the $V_{Nb}^{-0.6}$ term will vary between cases. (The variation in LNAPL molar volumes in Scenarios 1–4 leads to variations in computed diffusion coefficients of around 30%.)

The LNAPL dissolution rate is given by

$$R_n^{\text{diss}} = \lambda_n \theta \rho_w \left(c_n^{\text{lim}} - c_n\right) H(S_n) \quad (9)$$

where λ_n (s^{-1}) is the dissolution rate constant for the LNAPL, c_n^{lim} (kg/kg) is the solubility limit of the LNAPL and $H(\cdot)$ is the Heaviside function. The formulation ensures that the solubility limit is never exceeded and that saturations remain positive, or zero. The dissolution rate constant is chosen to be large to mimic pseudo-instantaneous dissolution. A value of 10^2 y^{-1} is used in all simulations.

LNAPL densities are taken to be constant in the model. The water density varies with the amount of dissolved LNAPL as

$$\rho_w = \rho_w^0 \left(1 + c^{\text{tds}} + c_n\right) \quad (10)$$

where ρ_w^0 (kg/m^3) is the density of water under in situ conditions and c^{tds} (kg/kg) is the concentration of any dissolved solids in the water.

3.3. Displacement pressure

A key control on the rate of migration of LNAPL through the waste package-backfill system is the threshold displacement pressure at which LNAPL is able to enter initially water saturated pores. The use of displacement pressures in models of LNAPL migration is complicated by the fact that it is a function of the intrinsic permeability of the package and backfill materials which, when considering the long-term evolution of materials in engineered barrier systems for radioactive waste, can vary over the modelling timescales.

To our knowledge, no directly relevant LNAPL–water displacement pressure data exist for the combination of the expected (phthalate-based) LNAPL types and specialised backfill material considered in this study. However, gas breakthrough pressures are available for a range of materials and provide a useful starting point because they are broadly equivalent to displacement pressures (Carruthers and Ringrose, 1998), although we acknowledge that the LNAPL–water displacement pressure may be lower. In order to scope the potential significance of LNAPL migration, we therefore started by estimating a gas displacement pressure and the using this to approximate the LNAPL–water displacement pressure for the modelled system by scaling the gas–water displacement pressure by the ratio of surface tensions. A useful survey of laboratory gas–water displacement pressures for a wide range of soil and rock types is given by Ingram et al. (1997) who determined the following power law regression relationship between displacement pressure and permeability:

$$p_{gd} = 6 \times 10^{-6} \left(\frac{1}{k}\right)^{0.33}. \quad (11)$$

Here, k is the intrinsic permeability of the media (m^2) and p_{gd} is the gas–water displacement pressure (MPa). The relationship was derived from approximately 100 reported values ranging over 12 orders of magnitude down to permeabilities of 10^{-23} m^2, with an appreciable scatter of up to an order of magnitude around the regression fit.

Directly applying Eq. (11) to the pristine package grout results in a threshold gas–water displacement pressure of around 2.4 MPa. The LNAPL–water displacement pressure can be approximated from the gas–water displacement pressure by scaling by σ_{wn}/σ_{wg}, where σ_{wn} and σ_{wg} are surface tensions (N/m) between the water and LNAPL, and water and gas, respectively. The water–gas surface tension is $\sigma_{wg} = 0.072$ N m^{-1}. Combining this with the water–LNAPL surface tension (Table 4) gives a scaling factor of 0.5 and therefore results in an approximate LNAPL–water displacement pressure of 1.2 MPa. This pressure was found to be sufficiently high to effectively prevent free phase (non-dissolved) LNAPL migration from the compacted waste pucks into the grout in all scenarios that were considered (the maximum amount of free phase LNAPL released from the pucks was less than 100 mg for the cases considered).

Since the direct applicability of the gas displacement pressure relationship (11) to the simulation of LNAPLs is uncertain it has not been used in this study. Instead, a bounding gas–water displacement pressure of $p_{gd} = 10$ Pa (scaling to give a LNAPL–water displacement pressure of $p_{nd} = 5$ Pa) was used in all of the scenarios that are considered. This is clearly smaller than Ingram's correlation would suggest, even taking the more extreme outliers in the data distribution, and represents a very conservative choice for p_{gd}. It effectively neglects the entry pressure barrier and thus overestimates the potential for LNAPL to enter the backfill and migrate away from the waste containers.

3.4. Model design

3.4.1. Model geometry

The simulated domain comprises a single 500 L annular-grouted waste package of the type shown in Fig. 1 surrounded by backfill extending to a height of 6 m above the waste package. This geometry is consistent with the assumption of the simulated waste package being the top-most package in the vault. The 6-m backfilled space corresponds to the region of the vault that is reserved for emplacement machinery during the emplacement operations, which is removed prior to backfilling. 50 cm of backfill is included to either side of the waste package. The overall geometry is shown in the left hand diagram in Fig. 5. An irregular cylindrical (r,z) grid is used to allow volumes near key interfaces in the system to be more finely resolved. The grid cell locations are visible in the right-hand diagram in Fig. 5, which shows the geometry local to the waste package. The waste package “walls” (the stainless steel container) are

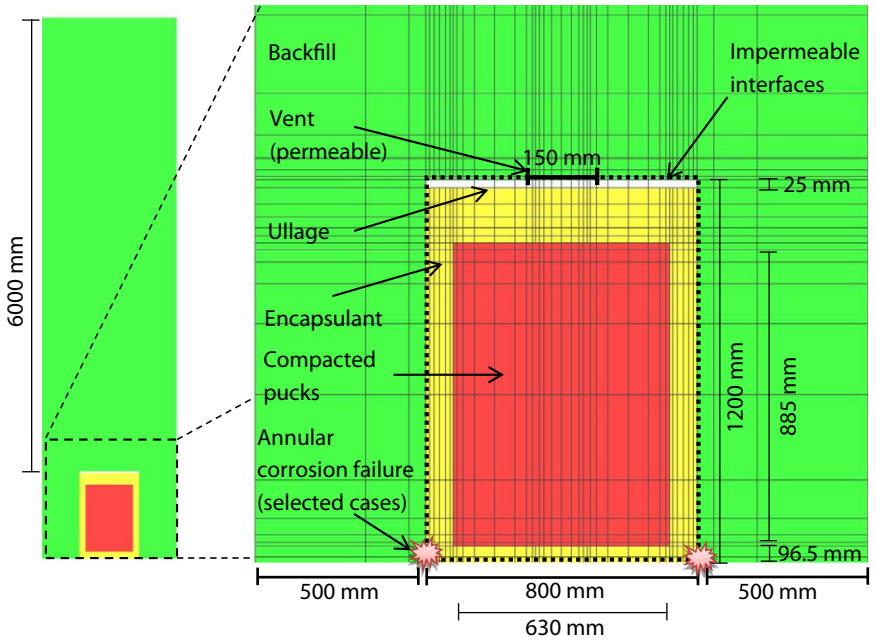

Fig. 5. Key dimensions of the waste package system. Left — entire domain simulated. Right — zoomed in view of waste package showing grid resolution and materials. Interfaces between encapsulant–backfill and ullage–backfill were set to be impermeable except for those in the vent, so that the vent provides to only pathway for LNAPL migration.

not included in the model. Instead, these are represented by impermeable interfaces between adjacent grid cells at the relevant locations. The only permeable interfaces surrounding the package in pristine (non-corroded) waste package scenarios are those representing the permeable vent at the top of the package. In corroded package scenarios the interfaces at the failure locations are set to be permeable, allowing flow through the package.

3.4.2. Boundary conditions

The system is initially assumed to be under hydrostatic conditions with a water pressure of $P_{top} = 6.5$ MPa at top of model. This gives pressures in the system of:

$$p = P_{top} + \rho_w g h \tag{13}$$

where h (m) is the vertical distance from the top of the simulated region. This pressure is assigned as the initial pressure in the system and is used to define the pressure boundary conditions on the pristine package model for the entire simulation time.

In scenarios where the waste package is assumed to be corroded (later Fig. 6), a pressure difference greater than the hydrostatic pressure difference is imposed between the top and bottom boundaries to give rise to a flow through the system in a bottom to top direction. RWMD's generic Disposal System Safety Case system model (NDA, 2010f) assumes a Darcy velocity in the higher strength host rock of 6×10^{-4} m/y. Since the simulated backfill is likely to be more permeable than the host rock, flow tends to focus through the backfill and this is represented through the use of a flow focussing factor. Whilst flows through the GDF as a whole may be dominantly horizontal, flows through the backfill between the low permeability waste stacks may be vertical (upwards at the upstream end of the vault and downwards at the downstream end of the vault) as water is focussed towards the more permeable backfilled region at the top of the vault. Since the main purpose of the imposed flows in the modelling discussion herein is to carry LNAPL away from the package, we have therefore imposed a vertical flow that will minimise the time taken for LNAPL to migrate to the top of the vault. The approach is hence conservative in this regard. Based on information in NDA (2010f), we have imposed a vertical Darcy velocity of 1.2×10^{-3} m/y through the waste stack. To approximate this in the model, a pressure difference was imposed between the top/bottom boundaries, which led to Darcy velocities in the model ranging from 1.18×10^{-3} m/y near the boundary with the host rock to 1.46×10^{-3} m/y at the sides of the waste package, where the flows are fastest.

On outflowing boundaries, in-situ LNAPL amounts are used to determine the fluxes out of the system. The neighbouring host rock is not represented in the model since a generic GDF design is being considered. Instead backfill properties are used to determine the fluxes. Proper representation of the host rock would be expected to provide an additional resistance to LNAPL migration out of the backfill due to the expected lower permeability of the rock. This would most likely cause any LNAPL that is able to migrate as far as the rock/backfill interface to accumulate there. Therefore all estimates of LNAPL migration out of the backfill are conservative in this respect. For any boundaries on which advective flow conditions evolve and are inwards (e.g. as a consequence of water flowing inwards to replace LNAPL that has migrated away), a LNAPL saturation of $S_N = 0$ (−) and water saturation of $S_w = 1$ (−) is assumed. The choice of $S_N = 0$ for LNAPL saturations on in-flowing boundaries ignores any 'interference' from LNAPL plumes emanating from neighbouring waste packages.

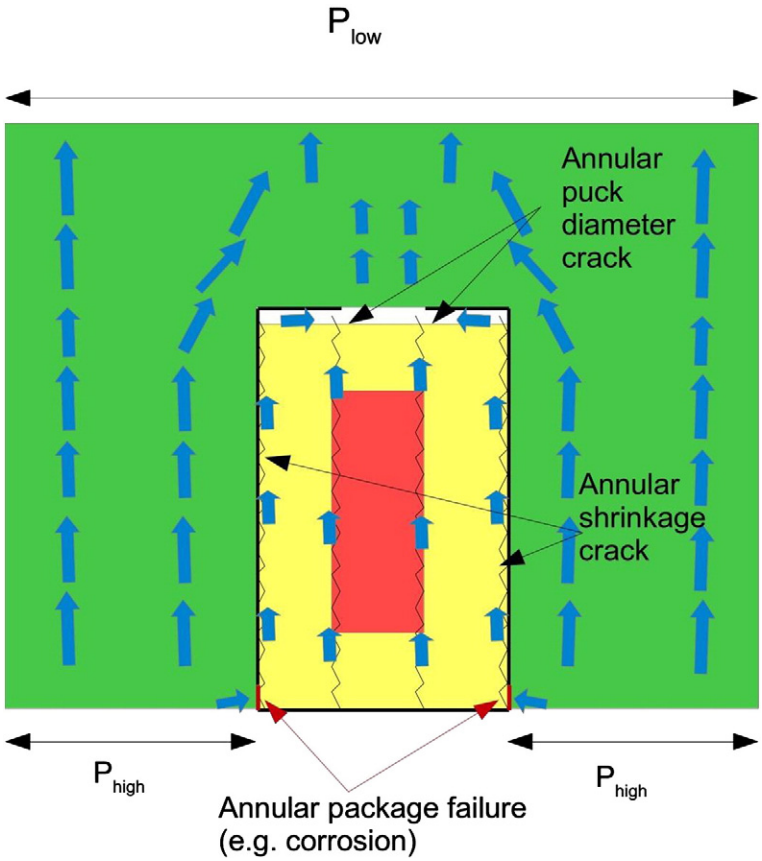

Fig. 6. Flow and corrosion/cracking concepts considered in the corroded encapsulant cases.

3.5. Scenarios and simulation cases

The migration of LNAPL from the compacted waste pucks, through the package grout and into the backfill via the ullage and vent (Fig. 5) is simulated for the LNAPL Scenarios 1–4 described in Table 2. Variant LNAPL scenarios have been developed to assess sensitivity of the evolution to LNAPL properties. Scenarios 2 and 3 include 'LS' (low solubility) and 'HS' (high solubility) variants that test the sensitivity of the evolution to the LNAPL solubility limit in the water. In the LS variant, the solubility limit is set to phthalate levels (0.3 mg/L) whereas in the HS variant, the solubility limit is set to a level that is more consistent with the inventory of 'other organics'. LNAPL Scenario 2 also includes '4V' and '4BC' variants designed to test sensitivity to LNAPL hydrogeological properties. In the '4V' variant, the sensitivity to LNAPL viscosity is assessed by setting the viscosity to the lower value of the Scenario 4 LNAPL and in the '4BC' variant, the hydraulic retention parameters (i.e. the Brooks–Corey parameters) of the Scenario 4 LNAPL is applied to the Scenario 2. These latter two variants are applied in conjunction with the higher solubility from the HS variant.

Three package scenarios are considered. The package is assumed to be either: intact (as-emplaced); to contain an internal annular crack in the grout connecting the top of the edge of the pucks to the ullage, but be otherwise intact; or corroded about an annulus at the base (as discussed in Section 3.4). These latter 'compromised package' scenarios are intended to represent the degradation of the package materials with time.

In the corroded package scenario, a groundwater pathway is established through the package and advection of Scenario 1 LNAPL can occur. The corroded package scenario includes three variant models of increasing levels of package failure, with increasing rates of advection: in the first, the interior of the package is assumed to be intact with no cracks in the grout; in the second, an annular shrinkage crack is assumed to have developed along the length of the grout/container interface where the grout is assumed to have shrunk away from the container; and in the third an additional annular crack is assumed to have developed in the grout at the puck radius, running from the bottom to the top of the package. The key features of the compromised package scenarios are sketched in Fig. 6.

A number of uncertain processes that would reduce the LNAPL release from the backfill have been neglected, as discussed earlier. Additionally, scoping calculations using a simple 'equivalent half-life' model for LNAPL degradation (Watson et al., 2012) suggest that the flux of LNAPL escaping the backfill will be significantly reduced if degradation of dissolved LNAPL can occur. The LNAPL degradation model and rate are uncertain and so any reduction in the LNAPL flux due to degradation in the dissolved phase has been ignored in the models that are presented. Similarly, sorption of dissolved LNAPL is ignored in the models. The package vent is likely to

Table 3
Material hydrogeological properties used in the modelling.

Property	Unit	Waste pucks	Package grout	Ullage	Fractures (if present)	Backfill
θ^0	(−)	0.05[a]	0.2	1.0	1.0	0.55
k	(m^2)	1E−13	1E−17	1E−11	1E−11	1E−15
τ	(−)	1.0	0.005	1.0	1.0	0.15
β	(Pa^{-1})	1E−15 (pseudo-incompressible assumption)				
k_w^{rel}	(−)	Linear with S_w	Brooks–Corey	1.0 (−)[b]	Linear with S_w	Brooks–Corey
k_n^{rel}	(−)	Linear with S_n	Brooks–Corey	1.0 (−)[b]	Linear with S_n	Brooks–Corey
p_{c_n}	(Pa)	0 Pa	Brooks–Corey (p_{nd} = 5 Pa)	0 Pa	0 Pa	Brooks–Corey (p_{nd} = 5 Pa)

[a] This is the porosity of the compacted pucks before LNAPL is released. Post-release porosities are used in the model and are calculated using the amount of LNAPL that is released in each scenario. The resulting porosities are 0.19, 0.23, 0.43 and 0.25 for Scenarios 1, 2, 3 and 4 respectively.
[b] Relative permeabilities of one have been set in the ullage for both water and LNAPL. Strictly, the sum of the relative permeabilities should be less than or equal to one but this is unlikely to have a significant effect on the results.

provide some resistance to flow, but since its hydraulic properties are not known precisely the vent is simulated as an open interface.

3.6. Scenario parameterisation

The hydrogeological parameterisation of the various materials included in the model are summarised in Table 3 and properties of the LNAPLs in each of LNAPL Scenarios 1–4 are summarised in Table 4. The geometry and dimensions of the system are shown in Fig. 5. Dimensions of the additional features that are present in the corroded package scenarios, together with their associated hydrogeological modelling assumptions, are given in Table 5.

In all simulations, the viscosity of water at 35 °C was taken to be $\mu_w = 7.2 \times 10^{-4}$ Pa s. At an assumed depth of 650 m, the concentration of dissolved solids in the water is likely to be around 0.02 kg/kg (Bond and Tweed, 1995). With no dissolved LNAPL, this results in a water density at in situ conditions in the model of around $\rho_w = 1017$ kg/m^3 (Eq. (11)). Thus LNAPLs in the system are those LNAPLs with density less than this value, and may include LNAPLs that are denser than pure water at STP (standard temperature and pressure).

4. Results and discussion

Results for the intact package scenarios are presented in Section 4.1, and results for the compromised package scenarios are presented in Section 4.2.

4.1. Intact waste package

The phenomenological evolution of the LNAPL in the intact package scenarios is illustrated by the snapshots of the free and dissolved LNAPL plume for LNAPL Scenarios 1 and 4 (Fig. 7). These are effectively the bounding cases in terms of the mobility of the free phase LNAPL with behaviour exhibited by the other scenarios falling within the envelope of these results.

Initially all the LNAPL is evenly distributed through the pucks, but within 100 y buoyancy of the LNAPL causes it to migrate vertically and accumulate at the top of the pucks. Since the hydraulic properties of the LNAPL in the pucks are the same in LNAPL Scenarios 1 and 4, the redistribution rate within pucks is similar. The rate at which the LNAPL then begins to migrate out of the pucks and through the grout and backfill is different. The Scenario 4 LNAPL breaks through the vent between 200 and 250 y, whereas the Scenario 1 LNAPL break though occurs much later between 4000 and 5000 y and at a lower rate. After 5000 y the Scenario 4 LNAPL reaches the interface with the host rock at the upper boundary and after 12,500 y almost all of the LNAPL (>95%) has migrated from the backfill via a narrow plume 'chimney'. There is little lateral spreading of the LNAPL plume since there is not a significant lateral pressure gradient and transverse dispersion is not represented in the model. In contrast, more than 99% of the Scenario 1 LNAPL is still present in the modelled system at 100,000 y and no breakthrough of free LNAPL at the upper boundary occurs.

Free phase LNAPL dissolves into the groundwater up to the relevant solubility limit wherever free phase LNAPL is present. As would be expected, there is more horizontal spreading in the dissolved phase plume and, due to the choice of boundary

Table 4
LNAPL properties in each scenario.

		Unit	1	2				3		4
				LS	HS	HS-4V	HS-4BC	LS	HS	
LNAPL mass per waste package		kg	38.9	47.4				95.1		47.4
ρ_n		kg/m^3	980	940				900		870
W_n		g/mol	405	255				303		226
$D_{n,pore}$[a]		m^2/s	5.8×10^{-10}	7.2×10^{-10}				6.6×10^{-10}		7.7×10^{-10}
μ_n		Pa s	8×10^{-2}	6.7×10^{-2}	6.7×10^{-2}	5×10^{-3}	6.7×10^{-2}	6.3×10^{-2}	6.3×10^{-2}	5×10^{-3}
c_n^{lim}		mg/L	0.3	0.3	89	89	89	0.3	61	100
Brooks–Corey	S_m	–	0.2	0.2	0.2	0.2	0.273	0.2	0.2	0.273
	m	–	0.7	0.7	0.7	0.7	0.85	0.7	0.7	0.85
	σ_{wn}	N/m	0.036	0.02	0.02	0.02	0.036	0.02	0.02	0.036

[a] Calculated using the Wilke–Chang formula (Eq. (9)) at 35 °C.

Table 5
Dimensions of additional features in corroded package scenarios and associated hydrogeological modelling assumptions.

Feature/property	Value/modelling details	Notes
Corroded area (if present)		
Total area	50 mm^2	Assumed value
Shrinkage crack (if present)		
Aperture	1 mm	Assumed value
Hydraulic model	$k_i^{rel} = S_i, p_{c_n} = 0$ Pa	Fractured media assumption
Puck crack (if present)		
Aperture	1.0 mm or 0.1 mm	Larger value used in non-corroded case
Hydraulic model	$k_i^{rel} = S_i, p_{c_n} = 0$ Pa	Fractured media assumption
Advective flow field		
Head gradient $(1 - \alpha)$	−0.0027	Results in $u_w \sim 1.2 \times 10^3$ m/y in backfill

conditions (Section 3.4.2), there is a flux of dissolved LNAPL out of the sides of the system whilst free phase LNAPL is present and continues to dissolve. Due to the mildly increased density of the dissolved LNAPL-rich water, dissolved LNAPL remains in the package after the free phase LNAPL has migrated away (in the case of LNAPL Scenario 4). This LNAPL diffuses slowly out of the package, with dissolved LNAPL still remaining in the package at close to the solubility limit at 100,000 y in both cases.

The difference in the degree of LNAPL migration is clearly a factor of the different LNAPL properties between Scenarios 1 and 4. The degree of migration seen in LNAPL Scenarios 2 and 3, whose properties are 'between' those of LNAPL Scenarios 1 and 4, will help to identify the key controls on the migration. For each of LNAPL Scenarios 1–4, the cumulative amounts of free phase LNAPL having passed through the vent are shown in Fig. 8a and cumulative amounts passing out of the boundary with the host rock at the top of the system are shown in Fig. 8b. Cumulative amounts of dissolved phase LNAPL out of all boundaries with the host rock are shown in Fig. 8c.

The flux of free phase LNAPL through the vent is larger in Scenario 4 than in any of the more realistic LNAPL Scenarios 1–3, with earlier LNAPL break through at the vent, at around 200 y, and subsequently shorter timescales for complete depletion of LNAPL from the package, at around 10,000 y. The only comparable case is the Scenario 2 HS-4V variant, in which the viscosity of the Scenario 4 LNAPL is used for the Scenario 2 LNAPL. In this case, the net fluxes are approximately half those of Scenario 4 and vent break through and depletion times are around 400 y and 20,000 y respectively.

This result suggests that the key differentiating factor between the Scenario 4 LNAPL and the Scenarios 1–3 LNAPLs, which leads to higher magnitude fluxes of free LNAPL, is the LNAPL viscosity. This is somewhat confirmed by the Scenario 2 HS-4BC variant in which the Brooks–Corey parameters for the Scenario 4 LNAPL are used with the Scenario 2 LNAPL. In this case results are almost indistinguishable from the Scenario 2 HS

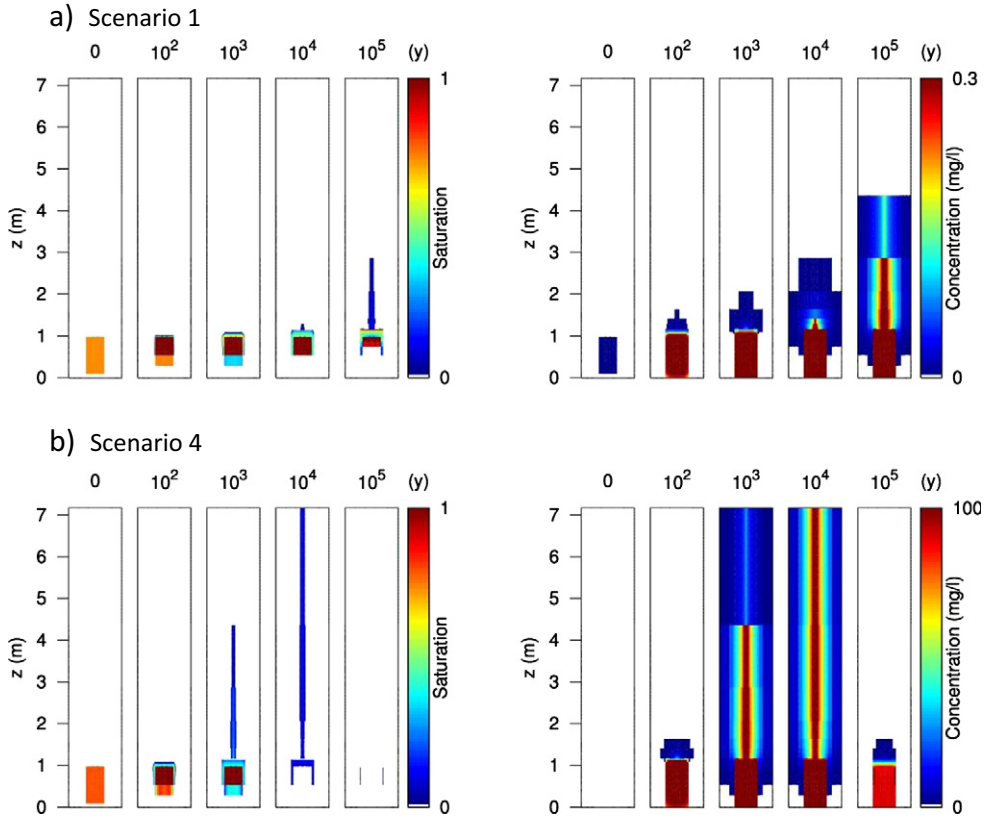

Fig. 7. Plumes of free LNAPL (left) and dissolved LNAPL (right) for the intact package LNAPL Scenarios 1 and 4 (shown within the entire Fig. 5 domain simulated).

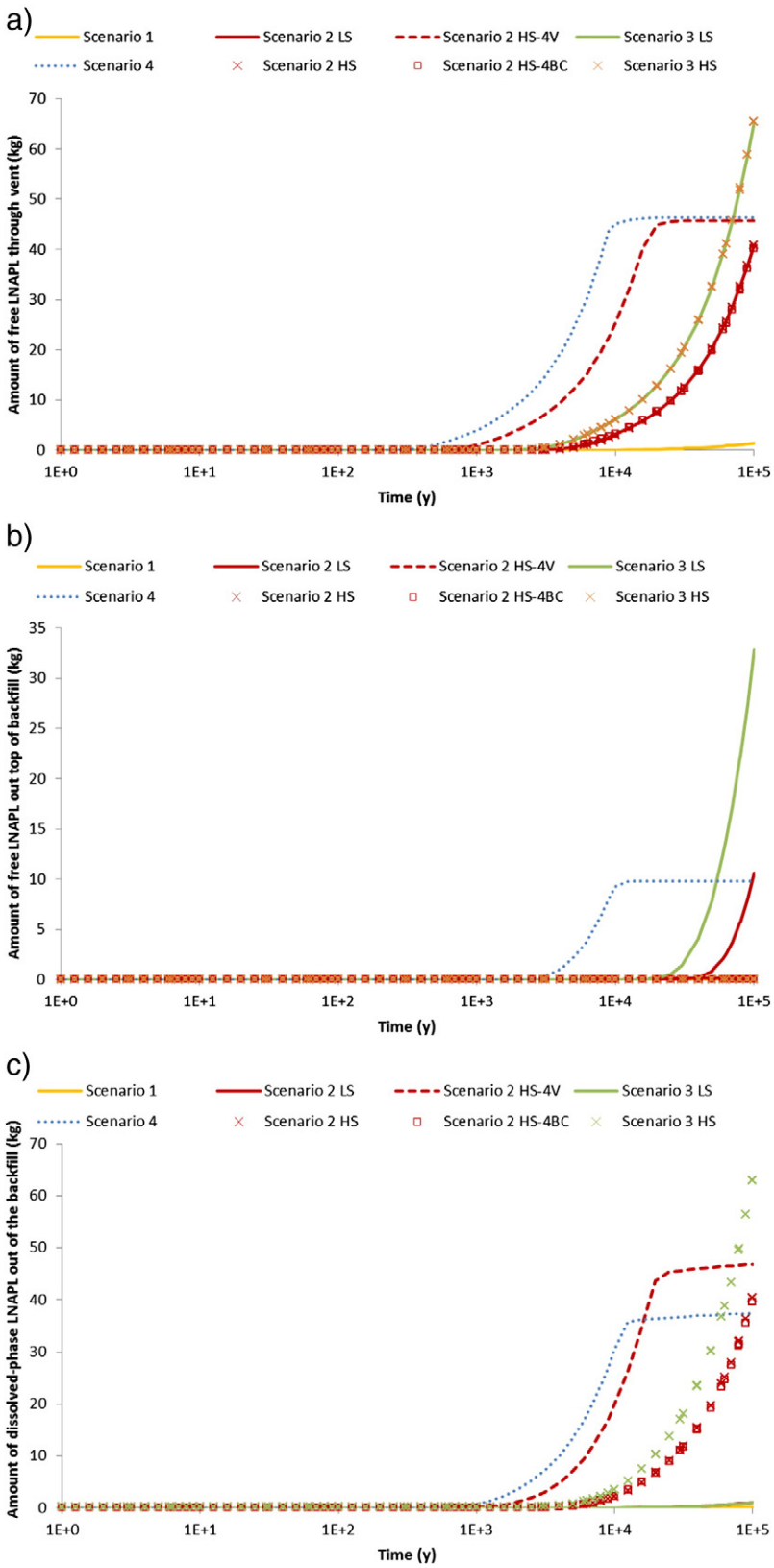

Fig. 8. Cumulative amounts of free phase LNAPL having (a) passed through the vent and (b) into the host rock at the top of the system; and (c) cumulative amounts of dissolved LNAPL leaving the system. Note that the initial inventory of LNAPL varies between the cases.

Table 6
Summary of key event timings and quantities, showing: time taken for free phase LNAPL breakthrough at the vent (T_{vent}) and the backfill/rock interface at the top of the system (T_{rock}); cumulative amount of free phase LNAPL passing through the vent (A^{free}_{rock}) and the backfill/rock interface at the top of the system (A^{free}_{rock}); cumulative amount of dissolved LNAPL passing through the backfill/rock interface at the top of the system (A^{diss}_{rock}); and either the time taken for 95% of the LNAPL to leave the system (T_{95}) or the fraction of the LNAPL remaining at 100,000 y ($F^{remain}_{100,000}$).

		T_{vent} (y)	T_{rock} (y)	A^{free}_{vent} (kg)	A^{free}_{rock} (kg)	A^{diss}_{rock} (kg)	T_{95} (y) or $F^{remain}_{100,000}$ (%)
Scenario 1		4000–5000	–	1.5	0	0.16	>99%
Scenario 2	LS	1585–1995	20,000–25,119	40.9	10.6	1.1	75%
	HS	2512–3000	–	40.7	0	40.2	15%
	HS-4V	400–500	9000–10,000	45.6	0.14	46.8	20,000–25,119 y
	HS-4BC	2000–2512	–	40.1	0	39.6	16%
Scenario 3	LS	1000–1259	12,589–15,489	65.4	32.8	1.1	64%
	HS	1259–1585	–	65.4	0	62.8	34%
Scenario 4		200–251	1585–1995	46.3	9.8	37.5	10,000–12,589 y

variant, suggesting that the differences in the Brooks–Corey parameters have little effect.

The Scenario 2 LS and HS variants highlight the role of the solubility limit in allowing LNAPL to leave the system in the dissolved phase. In both cases around 41 kg of free phase LNAPL migrates through the package vent in the 100,000 y simulation time. In the HS variant almost this entire amount of LNAPL subsequently leaves the system in the dissolved phase, whereas in the LS variant the amount of dissolved LNAPL leaving the system is only 1.1 kg, with 10 kg of the undissolved free phase LNAPL managing to migrate to the host rock above.

The only cases in which a non-trivial flux of free LNAPL out of the backfill and into the host rock at the top of the system arises are the (unrealistic LNAPL) Scenario 4 and Scenarios 2 LS and 3 LS (Fig. 8b). As noted above, the higher solubility variants tend to lead to LNAPL migration in the dissolved phase and almost complete removal of free phase LNAPL. The highly mobile Scenario 4 LNAPL has a high solubility, but its flux through the vent and into the backfill is sufficiently large that it exceeds the rate at which free LNAPL is lost to the dissolved phase and so LNAPL is able to migrate from the backfill in the free phase in this case. As also noted above, LNAPL Scenario 2 HS-4V has a flux of approximately half that of Scenario 4, but in this case no LNAPL migrates in the free phase because the flux in this case is below the critical rate required to exceed the rate of dissolution over the 6 m path length to the top of the system. If a shorter backfill pathway were present then it is likely that free phase LNAPL would also migrate from the system in this case.

A summary of the timing of key events and details of key quantities in the evolution of LNAPL Scenarios 1-4 is given in Table 6.

4.2. Compromised waste package cases

Compromised package variant scenarios were run for the Scenario 1 LNAPL (arguably the most realistic LNAPL of the 2D03 wastestream, Section 2.7). Fig. 9 shows the results from the compromised package scenario where a puck crack is assumed to be present, but where no package corrosion has occurred. In this case the thickness of the crack at the puck radius is 1 mm. Fig. 9a shows the modified grid used in this case; 1 mm thick cells are used to explicitly represent the fractured region. The breakthrough of free phase LNAPL at the vent is shown in the free LNAPL flux plot Fig. 9b. Results from the intact package LNAPL Scenario 1 are shown for comparison. When the puck crack is present the breakthrough at the vent is almost immediate (<1 y), compared to the breakthrough time of around 5000 y in the intact package case. For a period of around 10 y the flux through the vent in the puck crack scenario is around 1 g/y, which is around 100 times larger than the flux through the vent in the intact package scenario. However by around 50 y it falls to the same 0.02 g/y rate as for the intact package case and the long-term (>10,000 y) evolution in both cases is almost identical.

The LNAPL fluxes through the vent converge to the same value in the two cases because once the ullage is saturated with LNAPL, the rate at which LNAPL can leave the package is controlled by the hydraulic resistance of the vent. As noted earlier, the models conservatively assume that the vent does not offer any additional resistance and so the resistance of the vent interface in the model corresponds to the hydraulic resistance between the (open) ullage and the backfill interface. This resistance is the same in both scenarios once the ullage becomes saturated. This would suggest that cases with cracks with varying apertures, or more cracks, would not be likely to lead to increased fluxes through the vent, and would only affect the time taken for the LNAPL to saturate the ullage.

Three compromised package scenarios that include a region of corrosion have been run. These are: a corroded package with no cracks; a corroded package with an annular shrinkage crack (1 mm); and a corroded package with an annular shrinkage crack (1 mm) and a puck crack (0.1 mm). The scenarios are referred to as “NC” (no cracks), “SC” (shrinkage crack) and “SCPC” (shrinkage crack, puck crack). The corrosion of the container leads to advection of the LNAPL in the groundwater pathway through the package, which is parameterised as described in Section 3.4.2. An additional scenario was run in which the advection boundary conditions were applied to the intact package scenario, to compare the effect of advection in the backfill (only) with the corresponding diffusion-only scenario (Section 4.1).

Fig. 10 shows the LNAPL saturation plots at either the simulation end time (100,000 y) or the time shortly before which the LNAPL had almost entirely migrated from the package (40,000, 50,000 and 2500 y for Scenarios NC, SC and SCPC respectively). All of the corroded package cases experienced numerical difficulties at this time that seemed to be caused by LNAPL saturations approaching zero in the relative permeability curves for the fractures and ullage as the packages approached complete depletion of LNAPL.

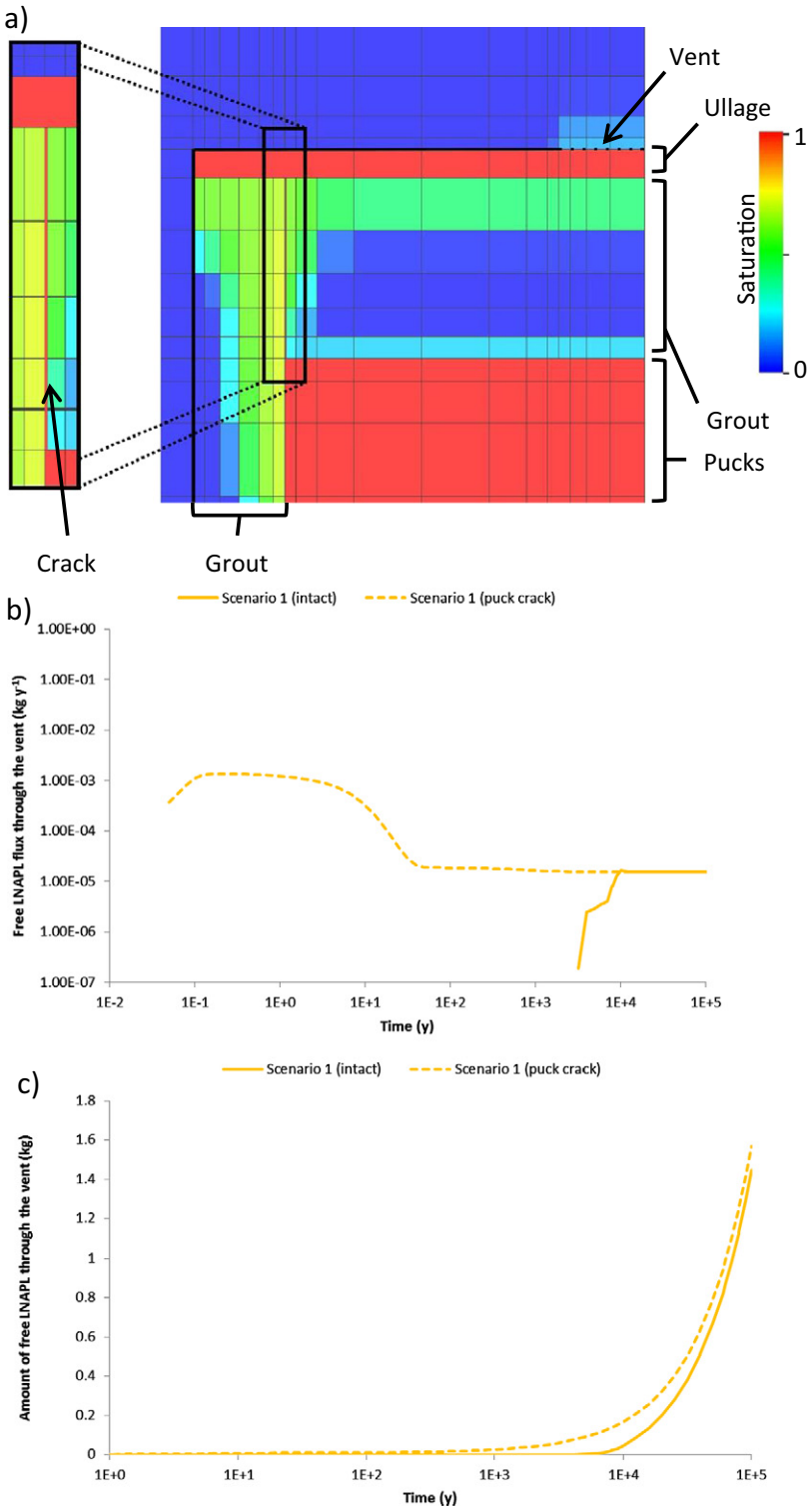

Fig. 9. Case 1 puck crack variant showing (a) plot of saturation at 1000 y (zoomed around puck crack cells); (b) free LNAPL flux through the vent; and, (c) cumulative amount of free LNAPL flux having passed through the vent.

Nevertheless, sufficient LNAPL migration through the package and into the backfill had occurred by this point in the simulations that useful conclusions can still be drawn.

Including advection in the backfill for the intact package scenario has little effect on the Scenario 1 LNAPL migration. The long timescales for migration within the package dominate

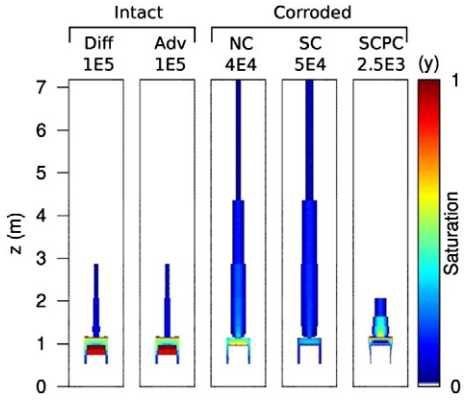

Fig. 10. Plumes of free LNAPL for the corroded package Scenarios NC, SC and SCPC at times shortly before complete LNAPL migration from the system (NC and SC) or shortly prior to breakdown of the numerical solve (SCPC). LNAPL plumes at 100,000 y for the intact package with and without advection are shown for comparison.

the release through the vent, and, given the low solubility of the LNAPL, the advective flow field in the backfill does not greatly affect the migration. The corroded package scenario with no cracks (NC) and with the shrinkage crack (SC) behaved similarly, with a large fraction of the LNAPL leaving the package in 40,000 y for scenario NC and 50,000 y for scenario SC, by which time respectively 65% and 82% of the initial inventory left the packages. In the SCPC scenario 39% of the initial inventory left the package by 2500 y.

The reason for the slow migration through the advective backfill is that the Scenario 1 LNAPL viscosity is approximately two orders of magnitude greater than that of water, which causes the free phase LNAPL plume to migrate more slowly than the surrounding water. Also, LNAPL migration in the backfill is limited by the need to maintain the LNAPL saturation throughout the LNAPL plume in the backfill at a value where the relative permeability and driving forces for migration (approximately) balance. This occurs at a LNAPL saturation of around 0.2, and acts as a temporary retarding mechanism on the LNAPL as it migrates through the backfill. The free phase LNAPL migration in the backfill is sufficiently slow that in all cases, almost all LNAPL leaving the backfill (where there was any) was in the dissolved phase.

The amounts of LNAPL that have migrated through the vent as a function of time in each case is shown in Fig. 11a and the total amount of LNAPL (free and dissolved) that has migrated out of the backfill is shown in Fig. 11b. In these plots an extrapolated estimate of LNAPL migration is plotted for the SCPC scenario, in which the LNAPL migrated out of the vent sufficiently quickly that the simulation faltered when zero saturations were approached inside the package before any significant migration through the backfill could occur. The approach to extrapolation is based on the observation that once LNAPL enters the backfill its migration is largely controlled by the hydraulic properties of the LNAPL in the backfill, and will only vary between cases if the rate of LNAPL release leads to locally elevated LNAPL saturations that increase the relative permeability. Therefore the estimate assumes that the amount of LNAPL that has migrated through the vent in the SCPC case, $a^{est}_{SCPC}(t)$ (kg), is related to the same quantity in the SC case, $a_{SC}(t)$ (kg) by:

$$a^{est}_{SCPC}(t) = a_{SC}(ct) \quad (14)$$

where c is a constant timescale factor. A value of $c = 4$ was been found to provide a reasonable fit to the calculated amount of LNAPL migration through the vent up to 2500 y.

The key behaviour in each of the corroded package scenarios is summarised in Table 7.

4.3. Discussion

The modelling results indicate that the viscosity is a key control on LNAPL migration release from a GDF. The Scenario 4 LNAPL is judged to be unrealistic and has an artificially high mobility when compared to the more realistic LNAPL Scenarios 1–3. It is likely that for realistic LNAPL compositions only small amounts of free phase LNAPL would migrate from an intact waste package even if there were cracks in the grout.

A critical ratio of flux of LNAPL through the vent to dissolution rate is required for free phase LNAPL to reach the top of the backfill column. The critical ratio is determined by the LNAPL flux through the vent, the solubility limit and the path length through the backfill. Free phase LNAPL migration to the host rock is less likely if vent fluxes are small, solubility limits are high and path lengths are long, although the capacity of the system to dissolve all of the free LNAPL will depend on groundwater availability. The unrealistically mobile Scenario 4 LNAPL appears to be close to this critical ratio since its flux is only twice as large as the Scenario 2 HS-4V LNAPL case for which free phase LNAPL does not reach the top of the backfill. Therefore 'more realistic' LNAPLs are generally likely to fall below this critical ratio meaning that free phase LNAPL would not reach the top of the disposal vault. The only pristine package scenarios in which free phase LNAPL reached the host rock in the scenarios considered were the low solubility variants.

Once LNAPL has passed through the vent, migration is controlled by the properties of the backfill. The relatively high viscosity of the LNAPL and the need to develop a sufficient LNAPL saturation to provide a significant relative permeability means that even in the corroded package cases where the package provides relatively little containment, little or no free-phase LNAPL reaches the top of the backfill for realistic LNAPL compositions

Various conservatisms are included in the models, of which the most significant are the small displacement pressure that is assumed, the use of the maximum possible initial inventory of LNAPL, the lack of any hydraulic resistance of the package vent and the lack of any degradation of dissolved LNAPL in the models. The small displacement pressure assumed in the modelling results in behaviour similar to that which might be expected were the backfill to contain fractures.

5. Conclusions

The evidence obtained from our review of the ILW LNAPL source term potential and numerical modelling of LNAPL potential release at the waste package–GDF scale, supports the proposition that the release of a discrete LNAPL phase from

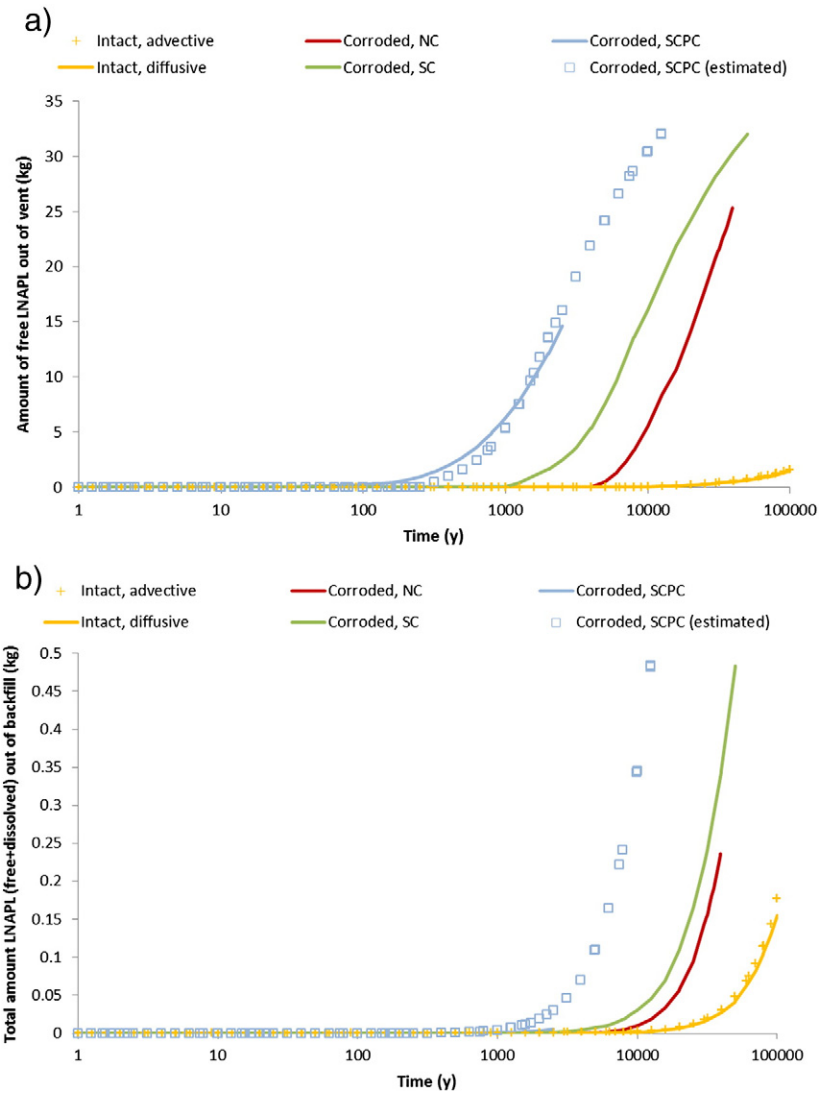

Fig. 11. (a) Amount of LNAPL that has migrated through the vent as a function of time in each of the corroded package scenarios; and, (b) amount of LNAPL (free + dissolved) that has migrated out of the backfill as a function of time in each of the corroded package scenarios; almost all of the LNAPL leaves the system in the dissolved phase in each case. Intact package scenarios (with and without advection in the backfill) are shown for comparison for (a) and (b).

disposed ILW waste packages is likely to be extremely limited and would not present a significant challenge to the safety case. 'As-disposed' LNAPL originally disposed within the ILW are extremely unlikely to be able to migrate from the waste package as a free phase, as: the disposability assessment process limits waste package LNAPL contents; waste forms are designed to immobilise and encapsulate LNAPL; and, LNAPL would be dispersed and immobile throughout the wasteform. Rather, our review of the ILW inventory and laboratory studies on degradation of organic materials present (mainly plastics) confirms the release of 'secondary LNAPL' arising from the in situ decomposition of disposed organic material, notably the halogenated plastic, PVC, may have the potential to form the predominant LNAPL source term. LNAPL generated from PVC, however, is expected to have very low buoyancy-based mobility, being a high molecular weight phthalate-based LNAPL of low density contrast with water and high viscosity.

Table 7
Percentages of initial LNAPL (free + dissolved) that have migrated through the vent ($F^{vent}_{10,000}$) and out of the backfill ($F^{backfill}_{10,000}$) by 10,000 y in the corroded package scenarios. Intact package scenarios results (with and without advection in the backfill) are shown for comparison.

Case	$F^{vent}_{10,000}$ (%)	$F^{backfill}_{10,000}$ (%)
Intact, diffusive	0.115	0.004
Intact, advective	0.120	0.004
Corroded, NC	14.2	0.03
Corroded, SC	41.2	0.08
Corroded, SCPC (estimated)	78.3	0.9

Numerical modelling was based around the 2D03 waste-stream, which is a high volume wastestream with elevated organic material–PVC content. It is packaged as an annular grouted wasteform, anticipated to be the least effective wasteform type for LNAPL containment. Predictions were

hence pessimistic compared to most other ILW wastestreams and package types. The models also adopted a range of other conservatisms (Section 4.3), the most significant being the small displacement pressure assumed and the maximum bounding inventory. Still, even with such conservatisms, the overall conclusion of the model simulations of intact and compromised (cracked and or corroded) waste packages for a range of realistic ILW LNAPL scenarios was that it is unlikely that significant LNAPL would be able to migrate from the waste packages and even more unlikely it would be sufficiently persistent to reach the top of the backfill and enter the host rock. Whilst the value of further refining of estimates of the LNAPL source term and reducing sensitive flow and transport parameter uncertainties is duly recognised, the conservative approach adopted herein suggests such further knowledge will not lead to any fundamental changes in the principal conclusions drawn. This conclusion, however, may need further consideration at a time when the UK Managing Radioactive Waste Safely process becomes site-specific, and data relating to an actual UK site are available to be used.

Finally, it is hence anticipated that assessment of potential LNAPL migration beyond the GDF within the wider geological barrier and biosphere is not warranted.

Acknowledgements

The research was funded by the Nuclear Decommissioning Authority Radioactive Waste Management Directorate (NDA RWMD), now Radioactive Waste Management Limited (RWM). Grainne Carpenter and Anthony Lansdell (formerly of Amec and now with NSG Environmental Ltd), in particular are acknowledged for their management and contributions to the research. The views expressed and conclusions drawn are those of the authors and do not necessarily represent those of RWM.

References

Altmann, S., 2008. 'Geo'chemical research: a key building block for nuclear waste disposal safety cases. J. Contam. Hydrol. 102, 174–179. http://dx.doi.org/10.1016/j.jconhyd.2008.09.012.

Askarieh, M.M., Harris, A.W., Wisbey, S.J., 1993. The potential impact of oil and other non-aqueous phase liquids (NAPLs) on the long-term management of radioactive wastes. icem03-4887. Proceedings of ICEM03: The 9th International Conference on Radioactive Waste Management and Environmental Remediation, September 21–23, 2003 http://dx.doi.org/10.1115/ICEM2003-4887.

Askarieh, M.M., Chambers, A.V., Daniel, F.B.D., Fitzgerald, P.L., Holtom, G.J., Pilkington, N.J., Rees, J.H., 2000. The chemical and microbial degradation of cellulose in the near field of a repository for radioactive wastes. Waste Manag. 20, 93–106. http://dx.doi.org/10.1016/S0956-053X(99)00275-5.

Baker, S., Green, A., Williams, S.J., 2003a. A Scoping Study of the distribution of radionuclides between alkaline solutions and non-aqueous phase liquids. SERCO/ERRA-0510 AEAT/R/NS/0617. (Available from) http://www.nda.gov.uk/documents/biblio/.

Baker, S., Green, A., Williams, S.J., 2003b. The potential uptake of plutonium from alkaline solution by Castrol Nucleol 520, Serco assurance report SA/ENV-0556. http://www.nda.gov.uk/documents/biblio/detail.cfm?fuseaction=search.view_doc&doc_id=4872.

Bond, K.A., Tweed, C.J., 1995. Groundwater compositions for the Borrowdale Volcanic Group, Boreholes 2, 4 and RCF3, Sellafield, evaluated using thermodynamic modelling. Nirex Report NSS/R310 (http://www.nda.gov.uk/documents/biblio/detail.cfm?fuseaction=search.view_doc&doc_id=3145).

Brooks, R.H., Corey, A.T., 1964. Hydraulic Properties of Porous Media. Colorado State University, Hydrogeology Papers, Fort Collins, Colorado (http://digitool.library.colostate.edu///exlibris/dtl/d3_1/apache_media/L2V4bGlicmlzL2R0bC9kM18xL2FwYWNoZV9tZWRpYS8xNTIyNTc=.pdf).

Carruthers, D., Ringrose, P., 1998. Secondary oil migration: oil–rock contact volumes, flow behaviours and rates. In: Parbell, J. (Ed.), Dating and Duration of Fluid Flow and Fluid–Rock Interaction. Geological Society Special Publication. No. 144, pp. 205–220.

Chambers, A.V., Cowper, M.M., Myatt, B.J., Williams, S.J., 2004. Further studies of plutonium uptake by non-aqueous phase liquids. Serco Reference: SA/ENV-0656. http://www.nda.gov.uk/documents/biblio/detail.cfm?fuseaction=search.view_doc&doc_id=5055.

Christensen, T.H., Bjerg, P.L., Banwart, S.A., Jakobsen, R., Heron, G., Albrechtsen, H. J., 2000. Characterization of redox conditions in groundwater contaminant plumes. J. Contam. Hydrol. 45 (3–4), 165–241. http://dx.doi.org/10.1016/S0169-7722(00)00109-1.

CL:AIRE, 2014. An illustrated handbook of LNAPL transport and fate in the subsurface. CL:AIRE, London 978-1-905046-24-9 (www.claire.co.uk/lnapl).

Craven, A., 2005. An examination of cemented oil samples. AEA Technology Report AEAT/R/NS/0766 Issue 2, March 2005 (http://www.nda.gov.uk/documents/biblio/detail.cfm?fuseaction=search.view_doc&doc_id=5099).

Dawson, J., 2012. The potential for non-aqueous phase liquid production from irradiated PVC and vinlyesterstyrene (VES); AMEC/PPE-1008/001; Issue 2. https://auth.nda.gov.uk/documents/biblio/upload/NAPL_from_PVCVES_FINAL_21_03.pdf.

Dawson, J., Magalhaes, S., 2012. The potential for non-aqueous phase liquid production in irradiated polymers. (SA/ENV/0997) http://www.nda.gov.uk/documents/biblio/upload/The-potential-for-NAPL-production-in-irradiated-polymers-updated-11July-2012.pdf.

Dawson, J., Schneider, S., 2002. Ageing of PVC cables in British Nuclear Power Generation Plant, (report produced for British Energy Generation Ltd NES/GNSR/5055), RDTec001/RadP, 2002.

Gerhard, J.I., Pang, T., Kueper, B.H., 2007. Time scales of DNAPL migration in sandy aquifers examined via numerical simulation. Ground Water 45 (2), 147–157. http://dx.doi.org/10.1111/j.1745-6584.2006.00269.x.

Grambow, B., 2008. Mobile fission and activation products in nuclear waste disposal. J. Contam. Hydrol. 102, 180–186. http://dx.doi.org/10.1016/j.jconhyd.2008.10.006.

Humphreys, P.N., Laws, A., Dawson, J., 2010. A review of cellulose degradation and the fate of degradation products under repository conditions. Serco Report SERCO/TAS/002274/001 (https://www.nda.gov.uk/documents/biblio/upload/A-Review-of-Cellulose-Degradation-and-the-fate-of-degradation-products-under-repository-conditions.pdf).

Hunter, F.M.I., Jackson, C.P., Kelly, M.J., Williams, S.J., 2006. A post-closure toxicity screening assessment for the Nirex Phased Geological Repository Concept. Serco Report SA/ENV/0854 (Available from http://www.nda.gov.uk/documents/biblio/).

Ingram, G.M., Urai, J.L., Naylor, M.A., 1997. Sealing processes and top seal assessment. In: Molle-Pedersen, P., Koestler, A.G. (Eds.), Hydrocarbon seals: importance for exploration and productionNorwegian Petroleum Society, Special Publication. 7. Elsevier, Amsterdam, pp. 165–174 (http://www.ged.rwth-aachen.de/files/publications/publication_378.pdf).

ITRC, 2009. Evaluating LNAPL Remedial Technologies for Achieving Project Goals. Interstate Technology and Regulatory Council, LNAPLs Team, Washington, DC (53 pp. http://www.itrcweb.org/Guidance/GetDocument?documentID=48).

Jonsson, S., Vavilin, V.A., Svensson, B.H., 2006. Phthalate hydrolysis under landfill conditions. Water Sci. Technol. 53 (8), 119–127 (http://www.iwaponline.com/wst/05308/wst053080119.htm).

Kirkman, A.J., Adamski, M., Hawthorne, J.M., 2012. Identification and assessment of confined and perched LNAPL conditions. Groundwater Monit. R. 33 (1), 75–86. http://dx.doi.org/10.1111/j.1745-6592.2012.01412.x.

Liang, D.-W., Zhang, T., Fang, H.H.P., He, J., 2008. Phthalates biodegradation in the environment. Appl. Microbiol. Biotechnol. 80, 183–198. http://dx.doi.org/10.1007/s00253-008-1548-5.

Mercer, J.W., Cohen, R.M., 1990. A review of immiscible fluids in the subsurface: properties, models, characterization and remediation. J. Contam. Hydrol. 6 (2), 107–163. http://dx.doi.org/10.1016/0169-7722(90)90043-G.

Montgomery, J.H., 2007. Groundwater Chemicals Desk Reference (Version 4 (and Earlier)). CRC Press 9781420009132 (1701 pp.).

NDA, 2007. Waste stream data sheet for 2D03, plutonium contaminated materials; drums. https://www.nda.gov.uk/ukinventory/_cs_upload/documents/Waste_Stream_Data_Sheets/Individual_WSDS/Sellafield_NDA/3095_1.pdf.

NDA (Nuclear Decommissioning Authority), 2010a. Geological disposal: gas status report, NDA/RWMD/037. https://www.nda.gov.uk/documents/upload/Geological-Disposal-Gas-status-report-December-2010.pdf.

NDA (Nuclear Decommissioning Authority), 2010b. Geological disposal: an overview of the generic disposal system safety case. (NDA/RWMD/010) https://www.nda.gov.uk/documents/upload/Geological-Disposal-An-overview-of-the-generic-Disposal-System-Safety-Case-December-2010.pdf.

NDA (Nuclear Decommissioning Authority), 2010c. Geological disposal: generic environmental safety case main report. NDA Report NDA/RWMD/021,

December 2010 (https://www.nda.gov.uk/documents/upload/Geological-Disposal-Generic-Environmental-Safety-Case-main-report-December-2010.pdf).
NDA (Nuclear Decommissioning Authority), 2010d. Geological disposal: generic disposal facility designs. NDA Report NDA/RWMD/048, December 2010 (https://www.nda.gov.uk/documents/upload/Geological-Disposal-Generic-disposal-facility-designs-December-2010.pdf).
NDA (Nuclear Decommissioning Authority), 2010e. Geological disposal: near field evolution status report. NDA Report NDA/RWMD/033, December 2010 (https://www.nda.gov.uk/documents/upload/Geological-Disposal-Near-field-evolution-status-report-December-2010.pdf).
NDA (Nuclear Decommissioning Authority), 2010f. Geological disposal: generic post-closure safety assessment. NDA Report NDA/RWMD/030, December 2010 (http://www.nda.gov.uk/documents/upload/Geological-Disposal-Generic-Post-closure-Safety-Assessment-December-2010.pdf).
NDA (Nuclear Decommissioning Authority), 2012. Geological disposal — summary of NAPL studies. (March 2010) NDA Technical Note No. 17779488 (http://www.nda.gov.uk/documents/biblio/upload/GD-Summary-of-NAPL-Studies-March-2010.pdf).
Newell, C.J., Acree, S.D., Ross, R.R., Huling, S.G., 1995. Light non aqueous phase liquids. USEPA Ground Water Issue EPA/540/S-95/500 (http://www.epa.gov/superfund/remedytech/tsp/download/lnapl.pdf).
Pöyry, 2010. Development of the Derived Inventory for ILW & LLW based on the 2007 UK Radioactive Waste Inventory. (November 2010) Pöyry Report No. 390685/12 (http://www.nda.gov.uk/documents/biblio/upload/Poyry-DI-ILW-LLW-Report-Final-Helius.pdf).
Quintessa, 2012. QPAC: Quintessa's general-purpose modelling software. Quintessa Report QRS-QPAC-11 March 2012 (www.quintessa.org/qpac-overview-report.pdf).
Reed, D.T., Molecke, M.A., 1993. Generation of volatile organic compounds by alpha particle degradation of WIPP plastic and rubber material; ANLI/CMT/CP-79852. http://dx.doi.org/10.1557/PROC-333-233.
Rees, J.H., Gould, L.J., Kelly, M., Pilkington, N.J., 2002. The impact of non-aqueous phase liquids on repository performance. Nirex Report AEAT/ERRA-0405 (Available from http://www.nda.gov.uk/documents/biblio/).
Schwarzenbach, R.P., Gschwend, P.M., Imboden, D.M., 1993. Environmental Organic Chemistry. Wiley-Interscience, London, http://dx.doi.org/10.1002/0471649643.
Smith, V., Magalhaes, S., Schneider, S., 2010. The role of PVC additives in the potential formation of NAPL. AMEC Report AMEC/PPE/2834/001 (http://www.nda.gov.uk/documents/biblio/upload/NDA-PVC-Review-_Jan-2013_Final.pdf).
Sorokin, D.Y., Janssen, A.J.H., Muyzer, G., 2012. Biodegradation potential of halo(alkali)philic prokaryotes. Crit. Rev. Environ. Sci. Technol. 42, 811–856. http://dx.doi.org/10.1080/10643389.2010.534037.
United Kingdom Nirex Limited, 2005. The viability of a phased geological repository concept for the long-term management of the UK's radioactive waste, Nirex Report N/122, November 2005. (Available from) http://www.nda.gov.uk/documents/biblio/.
Watson, S., Benbow, S., Chittenden, N., Lansdell, A., Rivett, M.O., Towler, G., 2012. Potential for buoyant non-aqueous phase liquid to migrate in the free phase from a GDF. RWMD Report 17698/TR/03 (230 pp. http://www.nda.gov.uk/customcf/Bibliography/front/lytebox.cfm?doc_id=6233).
Wealthall, G.P., 2002. Migration of NAPLs in the geosphere: implications for repository performance. BGS Report CR/02/284 (Available from http://www.nda.gov.uk/documents/biblio/).
Wilke, C.R., Chang, P., 1955. Correlation of diffusion coefficients in dilute solutions. Am. Inst. Chem. Eng. J. 1, 264–270. http://dx.doi.org/10.1002/aic.690010222.
Wolfe, N.L., Burns, L.A., Steen, W.C., 1980a. Use of linear free-energy relationships and an evaluative model to assess the fate and transport of phthalate esters in the aquatic environment. Chemosphere 9, 393–402. http://dx.doi.org/10.1016/0045-6535(80)90022-3.
Wolfe, N.L., Steen, W.C., Burns, L.A., 1980b. Phthalate ester hydrolysis: linear free energy relationships. Chemosphere 9 (7–8), 403–408. http://dx.doi.org/10.1016/0045-6535(80)90023-5.